



FACULTY OF SCIENCE AND TECHNOLOGY

MASTER THESIS

Study programme/specialisation:

Spring semester, 2021

Konstruksjoner og materialer /
Master of Science in Engineering
Structures and Materials

Open

Author: Magnus Rokne Vågen

Programme coordinator: Gerhard Ersdal

Supervisor(s): Mostafa Ahmed Atteya

Master thesis title: Numerical evaluation of the axial capacity of cracked tubular members

Credits: 30

Keywords: Buckling of columns
Cracks
Non-linear finite element
analysis
NORSOK N-004
DNVGL-RP-C208

Number of pages: 39
+ appendices/other: 1 appendix (14 pages)

Stavanger, 15.06.2021
date/year

Acknowledgements

This thesis is the final project of the Master of Science in Engineering Structures and Materials at the University of Stavanger (UiS), worth 30 credits (ECTS). The master's thesis is a mandatory work carried out in the last semester of study to obtain a master's degree in Engineering Structures and Materials.

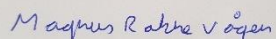
I would like to give a big thanks to my supervisor, Professor Gerhard Ersdal from UiS, for following me up by regular meetings during the process of the thesis work. His knowledge about buckling theory and his interest in numerical analysis has motivated me. I am grateful for all the guidance regarding the structure of the thesis.

I would like to thank my supervisor Mostafa Ahmed Atteya at UiS. His knowledge about non-linear finite element analysis and the finite element program Abaqus has been an enormous help in the thesis work. I am thankful for all discussions about the different numerical models and all useful tip and trick in Abaqus.

I will also give a huge thanks to my family and friends for believing in me and supporting me during the thesis work.

Stavanger, 15.06.2021

Magnus Rokne Vågen



Abstract

The objective of this thesis is to evaluate the axial capacity of cracked tubular elements analytically and numerically and compare these with laboratory tests. The laboratory tests have been performed by a different student and the experiments as such is not a part of this master thesis work.

The analytical hand calculations have been performed according to NORSOK N-004 and the numerical finite element analysis have been performed according to DNVGL-RP-C208.

In addition, two literature studies have been performed, one on non-linear finite element analysis and one on buckling of columns.

The numerical model used considers the same geometry used in the experimental work, non-linear stress-strain behaviour, and initial geometric imperfection. Four different models have been created, one undamaged column as a reference model and three damaged columns with different crack sizes. The crack sizes are 12%, 23,5% and 38,5% and the crack size is defined as the percentage of the circumference. Material properties such as Young's modulus and yield stress are obtained from the experimental work. Three types of boundary conditions are used, fixed-hinged, pinned-pinned, fixed-fixed, and the fixed-hinged boundary conditions related to the setup in the experimental test machine. Pinned-pinned and fixed-fixed are related to the buckling shape. The comparison between the experimental work and the fixed-hinged analysis has a good match in the calculated axial capacity, and its 2% – 7% differences in the capacity

The same four models that were used in the numerical model are used in the analytical hand calculations. The analytical hand calculations are performed by NORSOK N-004 and give an axial capacity of 13% lower than the experimental work for an undamaged column. This is more or less the same when the analytically calculations are compared with the non-linear finite element analysis.

The results show that there is a good match between the experimental work and the non-linear analysis. Some bigger differences are found in the comparison between the analytical results and the experimental work. This project ends with suggestions for further works.

Table of Contents

ACKNOWLEDGEMENTS	II
ABSTRACT	III
1 INTRODUCTION.....	1
1.1 BACKGROUND AND MOTIVATION	1
1.2 PROBLEM DESCRIPTION / THESIS OVERVIEW	1
1.3 LIMITATIONS.....	1
2 THEORY.....	2
2.1 INTRODUCTION.....	2
2.2 THEORY FOR GLOBAL BUCKLING OF COLUMNS.....	2
2.3 LOCAL BUCKLING OF COLUMNS	4
2.4 NON-LINEAR FINITE ELEMENT ANALYSIS	4
2.4.1 <i>Nonlinearity</i>	4
2.4.2 <i>Solvers</i>	4
3 STANDARDS FOR CAPACITY OF COLUMNS	7
3.1 INTRODUCTION.....	7
3.2 NORSOK N-004.....	7
4 NUMERICAL MODEL.....	14
4.1 INTRODUCTION.....	14
4.2 METHODOLOGY.....	14
4.3 ANALYSIS PROCEDURE – PRE-PROCESSING.....	15
4.3.1 <i>Software</i>	15
4.3.2 <i>Geometry</i>	15
4.3.3 <i>Mesh</i>	17
4.3.4 <i>Material modelling</i>	18
4.3.5 <i>Boundary conditions</i>	19
4.3.6 <i>Load application</i>	20
4.4 ANALYSIS PROCEDURE – PROCESSING.....	20
4.4.1 <i>Analysis method</i>	20
4.5 ANALYSIS PROCEDURE – POST-PROCESSING.....	21
4.5.1 <i>Imperfections (imperfections shape – magnitude)</i>	21
4.5.2 <i>Postbuckling analysis</i>	21
4.6 RESULTS.....	22
4.6.1 <i>Fixed-hinged boundary conditions</i>	22
4.6.2 <i>Pinned-pinned boundary conditions</i>	23
4.6.3 <i>Fixed-fixed boundary conditions</i>	25
5 COMPARISON AND DISCUSSION	27
5.1 INTRODUCTION.....	27
5.2 NON-LINEAR FINITE ELEMENT METHOD	27
5.2.1 <i>Fixed-hinged boundary conditions</i>	27
5.2.2 <i>Pinned-pinned boundary conditions</i>	29
5.2.3 <i>Fixed-fixed boundary conditions</i>	30
5.3 EXPERIMENTAL RESULTS	32
5.4 NORSOK N-004.....	34

6	CONCLUSION AND FURTHER WORK	37
6.1	CONCLUSION	37
6.2	SUGGESTED FURTHER WORK	37
7	REFERENCES.....	38

Table of Figures

Figure 4-1:	Samples cross-section [13].	15
Figure 4-2:	Samples test setup and crack definition.....	16
Figure 4-3:	Reference model.	16
Figure 4-4:	12% crack (left), 23,5% crack (middle) and 38,5% crack (right).....	17
Figure 4-5:	Meshed tubular element.....	17
Figure 4-6:	Local seeds introduced in the numerical model with 12% crack.	17
Figure 4-7:	Yields surface and isotropic hardening.....	19
Figure 4-8:	Boundary conditions case 1 (fixed-hinged).....	19
Figure 4-9:	Load applied at the top of the models.....	20
Figure 4-10:	Buckling shape of column with fixed-pinned boundary conditions.	22
Figure 4-11:	Buckling shape of column with pinned-pinned boundary conditions.	23
Figure 4-12:	Buckling shape of column with pinned-pinned boundary conditions.	25

List of Tables

Table 4-1:	Geometry properties.....	16
Table 4-2:	Material properties.	18
Table 4-3:	Formula for converting from "engineering" stress-strain to "true" stress-strain. Bottom left = formula (6), bottom right = formula (7). Reference [9].....	18
Table 4-4:	"True" stress and true "strain" after using eq. 6 and eq7 in DNV-RP-C208 [9].	18
Table 4-5:	Results from non-linear finite element analysis with positive and negative scale factor equal to 1.5. Boundary conditions: fixed-pinned.	22
Table 4-6:	Results from non-linear finite element analysis with positive and negative scale factor equal to 1.8. Boundary conditions: fixed-pinned.	22
Table 4-7:	Results from non-linear finite element analysis with positive and negative scale factor equal to 2.0. Boundary conditions: fixed-pinned.	23
Table 4-8:	Results from non-linear finite element analysis with positive and negative scale factor equal to 1.5. Boundary conditions: pinned-pinned.....	23
Table 4-9:	Results from non-linear finite element analysis with positive and negative scale factor equal to 1.8. Boundary conditions: pinned-pinned.....	24
Table 4-10:	Results from non-linear finite element analysis with positive and negative scale factor equal to 2.0. Boundary conditions: pinned-pinned.	24
Table 4-11:	Results from non-linear finite element analysis with positive and negative scale factor equal to 1.5. Boundary conditions: fixed-fixed.	25
Table 4-12:	Results from non-linear finite element analysis with positive and negative scale factor equal to 1.8. Boundary conditions: fixed-fixed.	25
Table 4-13:	Results from non-linear finite element analysis with positive and negative scale factor equal to 2.0. Boundary conditions: fixed-fixed.	26

Table 5-1: Results from non-linear finite element analysis with positive and negative scale factor equal to 1.5. Boundary conditions: fixed-hinged.	27
Table 5-2: Results from non-linear finite element analysis with positive and negative scale factor equal to 1.8. Boundary conditions: fixed-hinged.	28
Table 5-3: Results from non-linear finite element analysis with positive and negative scale factor equal to 2.0. Boundary conditions: fixed-hinged.	28
Table 5-4: Results from non-linear finite element analysis with positive and negative scale factor equal to 1.5. Boundary conditions: pinned-pinned.....	29
Table 5-5: Results from non-linear finite element analysis with positive and negative scale factor equal to 1.8. Boundary conditions: pinned-pinned.....	29
Table 5-6: Results from non-linear finite element analysis with positive and negative scale factor equal to 2.0. Boundary conditions: pinned-pinned.....	30
Table 5-7: Results from non-linear finite element analysis with positive and negative scale factor equal to 1.5. Boundary conditions: fixed-fixed.	31
Table 5-8: Results from non-linear finite element analysis with positive and negative scale factor equal to 1.8. Boundary conditions: fixed-fixed.	31
Table 5-9: Results from non-linear finite element analysis with positive and negative scale factor equal to 2.0. Boundary conditions: fixed-fixed.	32
Table 5-10: Experimental [11] and non-linear finite element results (fixed-hinged) and the ratio between the results.....	32
Table 5-11: Experimental [11] and non-linear finite element results (fixed-fixed) and the ratio between the results.	33
Table 5-12: Experimental [11] and non-linear finite element results (pinned-pinned) and the ratio between the results.....	33
Table 5-13: Results from NORSOK N-004 and the experimental work [11] and ratio between the results.....	34
Table 5-14: Results from NORSOK N-004 and non-linear finite element analysis (fixed-hinged) and ratio between the results.	35
Table 5-15: Results from NORSOK N-004 and non-linear finite element analysis (pinned-pinned) and ratio between the results.	35
Table 5-16: Results from NORSOK N-004 and non-linear finite element analysis (fixed-fixed) and ratio between the results.....	36

1 Introduction

1.1 *Background and motivation*

During a structural element's life, different types of failures can occur such as cracking, corrosion and fatigue. A finite element analysis can be used to calculate the capacity of a cracked column. In addition to finite element programs, different guidance's such as NORSOK N-004 can be used. NORSOK N-004 meets the expectations for safety for Norwegian petroleum activities. Physical behaviours in experimental work when failures occur are also of interest.

Several finite element programs can be used for performing a buckling analysis, Abaqus and Ansys are two commonly known programs that can do this type of analysis. In this thesis, Abaqus has been chosen. These types of programs are based on a finite element method. Some requirements are necessary for performing a non-linear analysis, and a "requirement guide" for a finite element analysis can be found in DNVGL-RP-C208 which are introduced in chapter 4.

Working in a finite element program has been interesting and have given me motivation. The process of modifying different parameters has resulted in progress, and that has been good.

1.2 *Problem description / thesis overview*

The objective of this thesis is to evaluate the axial capacity of cracked tubular elements analytically and numerically and compare these with laboratory tests. The laboratory tests will be performed simultaneously by a different student and the experiments as such is not a part of this master thesis work.

The analytical hand calculations will be performed according to the NORSOK N-004 and the numerical finite element analysis will be performed according to DNVGL-RP-C208. The basis for the analytical methods will be investigated and possibly be elaborated as part of this thesis.

In addition, two literature studies will be performed. The first literature study will be general about non-linear finite element analysis. The second literature study will be on buckling of columns.

1.3 *Limitations*

The crack development in an undamaged tubular element is not investigated in this project work, and the geometry is simple. Some simplification for the crack has also been considered such as no stresses in the crack. There have been done a small selection of crack sizes, three different cracks have been chosen. In addition, it has been added perfect circular holes to the ends of the cracks. Several things can be investigated on a column, but it's limited to only check the axial compression capacity.

2 Theory

2.1 Introduction

Global buckling and local buckling are two well known phenomena when it's come to the buckling of columns. Buckling leads to structural failures. Local and global buckling theory will be described in this chapter. A non-linear finite element analysis is based on a finite element method and it's necessary to know if the problem having nonlinearity behaviours. The nonlinearity and different types of solver will also be described in this chapter. Different types of solver such as Newton-Raphson, modified Newton-Raphson and the Riks method will be described in this chapter.

2.2 Theory for global buckling of columns

Buckling of columns is a well-known phenomenon in structural engineering and can lead to structural failure. Historically, several structural accidents and disasters have occurred due to buckling and instability. Buckling of an ideal column is traditionally seen as a stability problem, where the column can experience a sudden lateral deflection at a certain compressive load. Leonard Euler (1707 – 1783) is a famous person when it comes to buckling. He was the first to solve an elastic instability problem and according to Timoshenko and Genre [1] following assumptions was made: an ideal column, perfectly straight, compression load applied in the centre. This resulted in an expression called Euler-formula:

$$P_{cr} = \frac{\pi^2 \cdot EI}{L_{eff}^2} = \frac{\pi^2 \cdot EI}{(k \cdot L)^2}, \quad (2.1)$$

where:

P_{cr} is the critical load / Euler's critical load,

E is the young's modulus,

I is the second moment of inertia,

L_{eff} is the effective length of the column,

k is a coefficient which gives the effective length,

L is the length of the column.

The compression capacity before buckling of an ideal column can be found with Euler's formula. When the compression load exceeds the critical load, the column starts to buckle. Either the lateral displacement can be large or small, this depends on how much more load is applied to the column and a stability problem occurs.

According to Boresi and Schmidt [2], a perfect column will in most cases have deviations from the ideal conditions and is called imperfect columns. Applying an eccentric load is a

common deviation. Small and large eccentricity influence how early the column starts to buckle. The slenderness of the column also affects the behaviour. With help of the slenderness ratio L/r (L is the length of the column and r is the radius of gyration), the slenderness can be defined. If the column has a large slenderness ratio Euler's formula gives an accurate estimate of the critical load [2].

The Perry-Robertson formula is another formula for the buckling capacity of columns. This formula includes the effect of eccentric loading and the initial curvature [3]. The Perry-Robertson formula is shown under [4]:

$$\frac{N}{N_d} + \frac{\frac{N \cdot (w_0 + e) \cdot 1}{1 - \frac{N}{N_e}}}{M_d} \leq 1.0, \quad (2.2)$$

where:

- N is axial compression loading,
- N_d is column buckling capacity,
- w_0 is the initial deformation,
- e is the eccentricity of the axial compression load,
- N_E is the Euler buckling capacity,
- M_d moment capacity.

Another formula for the buckling capacity of columns is the Johnson-Ostenfeld approach and is commonly used in the engineering industry. This empirical approach takes the effect of plasticity into account and results in "elastic-plastic" buckling [5]. An expression for the Johnson-Ostenfeld can be found in the COTech paper "Buckling capacity of simulated patch corroded tubular columns – laboratory tests" [4]. The expression is shown under:

$$f_{cr} = \phi \cdot f_y, \quad (2.3)$$

$$\phi = \begin{cases} 1 - \frac{\lambda^2}{2}, & \lambda^2 \leq 2 \\ \frac{1}{\lambda^2}, & \lambda^2 \geq 2 \end{cases}, \quad (4)$$

where:

- $\lambda^2 = \frac{f_y}{f_E}$ is the slenderness,
- $f_E = \frac{N_E}{A}$ is the Euler buckling stress,
- f_y is the yield stress.

2.3 Local buckling of columns

Another phenomenon in structural engineering is the failure mode local buckling and how the capacity is affected. Local buckling occurs in structural elements such as thin-walled columns and leads to small deformations. Because of local buckling, the buckling capacity with these failures must be calculated and gives a lower capacity than for global buckling. Luckily, it's several things to do for avoiding these failures. For example, change element type, another geometry or thicker "column walls". The local buckling doesn't need to mean it's wrong to use the planned element because of the lower capacity.

2.4 Non-linear finite element analysis

In structural mechanics, nonlinearity can be divided into the following types: material nonlinearity, contact nonlinearity, and geometric nonlinearity. Most of the engineering problems can be described with complicated differential equations and numerical methods are a good tool [6]. Numerical methods are used for solving nonlinearity problems and it's common to use software for the calculations. Some of the common software solves the problems with the finite element method. Different types of solver such as

2.4.1 Nonlinearity

There are three types of non-linearities in a non-linear finite element analysis, namely:

- Material nonlinearity: When the material behaviour is described with both elasticity and plasticity the element has nonlinear material properties. The "stress-strain" relation can't be described linearly. The plastic behaviour keeps the deformation after unloading it. The "stress-strain" relation is difficult to describe simply, therefore the "stress-strain" rate is used which is called elastoplasticity. Viscoelasticity which is a time-dependent behaviour is another material nonlinearity [6].
- Contact nonlinearity: The contact nonlinearity occurs when two surfaces encounter each other. For example, when two objects push each other's.
- Geometric nonlinearity: If the structural element is exposed to a large load and the geometry changes because of large deformations, it's a geometric nonlinearity.

In Abaqus, all these types of non-linearity are possible to include. However, in this thesis contact non-linearities are not used.

2.4.2 Solvers

A numerical method based on iterations with converge criteria is normally used for solving non-linear problems. Two well know approaches are the Newton-Raphson method and the modified Newton-Raphson method. The Newton-Raphson method is load controlled method that uses iterations until the converge criteria are achieved for each load and gives an accurate

result. The displacement control method is a useful if a constant displacement is interesting to investigate. Another type of solvers is the Riks method also know as an arch-length method.

The numerical method Newton-Raphson solves non-linear equations and finds the roots. A force is applied and for finding the corresponding displacement several iterations are done. When the converge criteria have been achieved the displacement for the applied load is found and this result is very precise. An allowed error is compared to the “exact” solution. The Newton-Raphson formula is as follow:

$$x_{n+1} = x_n - \frac{f(x_n)}{f'(x_n)}, \quad (2.5)$$

For a complex non-linear equation, the true solution is hard to describe. If the true solution can be found equation 6 can be used for finding the error.

$$X_{error} = x_{true} - x_n, \quad (2.6)$$

In non-linear finite element analysis, the formula is different. An initial tangent stiffness and a force error are introduced. Following equations are used [7]:

$$k_{tn-1}\Delta u = \Delta P_n \rightarrow \Delta u_n = k_{tn-1}^{-1}\Delta P_n, \quad (2.7)$$

$$u_n = u_{n-1} + \Delta u_n, \quad (2.8)$$

where:

- k_{tn-1} is the initial tangent stiffness,
- Δu_n is the displacement increment,
- ΔP_n is the initial load increment,
- u_n is the current estimated displacement,
- u_{n-1} is the “previous” estimated displacement.

$$e_{pn} = P_n - ku_n, \quad (2.9)$$

where:

- e_{pn} is the current force error / load imbalance,
- P_n is the applied load,
- $k = k(u)$ is evaluated using displacement u_n ,
- u_n is current displacement.

Often a modification of the Newton-Raphson method is used for saving time during the analysis. Instead of calculating a new stiffness matrix for each increment, the modified Newton-Raphson method uses a new stiffness matrix when the load is changed. Despite this

method require more iterations, the calculation time is less than the normal Newton-Raphson method [7].

Another non-linear method is the Riks method known as the “Arc Length” method. This load-deflecting analysis includes the load magnitude as a variable. The problem can either be stable or unstable and the method works. Some assumptions are considered such as the load is proportional, and bifurcations do not occur.

3 Standards for capacity of columns

3.1 Introduction

There are several methods to calculate the capacity of a column. In a design situation, the most common method is to use a relevant standard. For example, NORSOK N-004 provides methods for calculations of columns that are intended to meet the expectations for safety in the regulations for the Norwegian petroleum activities. In this chapter, an overview of the NORSOK N-004 Standard is provided.

3.2 NORSOK N-004

The NORSOK N-004 standard can be used to calculate the capacity of a tubular element affected for different scenarios. Axial compression, bending and hydrostatic pressure are examples of investigations that can be done. In the 2004 versions of NORSOK N-004 [8] it's included formulas for calculations of damaged members. For later versions, NORSOK N-004 refer to N-006.

It's commonly using a reference element when buckling investigations are performed. This is for having something to compare the results from damaged columns with. The formulas for buckling capacity calculations of an undamaged column are presented first. Following formulas are used and they are found in NORSOK N-004 [8]:

$$N_{sd} \leq N_{c,Rd} = \frac{Af_c}{\gamma_M}, \quad (3.1)$$

where:

- N_{sd} is the design axial force,
- $N_{c,Rd}$ is the design axial compressive resistance,
- A is the cross sectional area,
- f_c is the characteristic axial compressive strength,
- γ_M is the material factor.

The characteristic axial compressive strength is calculated as follow:

$$f_c = \begin{cases} [1.0 - 0.28\bar{\lambda}^2]f_y, & \text{for } \bar{\lambda} \leq 1.34 \\ \frac{0.9 \cdot f_y}{\bar{\lambda}^2}, & \text{for } \bar{\lambda} \geq 1.34 \end{cases}, \quad (3.2)$$

where:

$\bar{\lambda}$ is the column slenderness parameter

f_y is the characteristic yield strength.

The column slenderness parameter is calculated as follow:

$$\bar{\lambda} = \sqrt{\frac{f_{cl}}{f_E}} = \frac{kl}{\pi i} \sqrt{\frac{f_{cl}}{E}}, \quad (3.3)$$

where:

f_{cl} is the characteristic local buckling strength,

f_E is the smaller Euler buckling strength in y or z direction,

k is the effective length factor,

l is the longer unbraced length in y or z direction,

i is the radius of gyration,

E is the Young's modulus of elasticity.

The characteristic local buckling strength is calculated as follow:

$$f_{cl} = \begin{cases} f_y, & \text{for } \frac{f_y}{f_{cle}} \leq 0.170 \\ \left(1.047 - \frac{0.274 \cdot f_y}{f_{cle}}\right) f_y, & \text{for } 0.170 \leq \frac{f_y}{f_{cle}} \leq 1.911, \\ f_{cle}, & \text{for } \frac{f_y}{f_{cle}} > 1.911 \end{cases}, \quad (3.4)$$

where:

f_y is the characteristic yield strength,

f_{cle} is the characteristic elastic local buckling strength.

The characteristic elastic local buckling strength (f_{cle}) is calculated as follow:

$$f_{cle} = \frac{2C_e E t}{D}, \quad (3.5)$$

where:

C_e is the critical elastic buckling coefficient = 0.3,

E is the Young's modulus of elasticity,

t is the wall thickness,

D is the outside diameter.

Different failures such as cracks can occur to the element. The formula for an undamaged tubular element is no longer valid. Therefore, a formula that takes the crack into account must be used. In NORSOK N-004 [8] following equations should be used for buckling capacity calculations with axial compression of a cracked element:

$$N_{sd} \leq N_{dent,c,Rd} = \frac{N_{dent,c}}{\gamma_M}, \quad (3.6)$$

where:

- N_{sd} is the design axial force,
- $N_{dent,c,Rd}$ is the design axial compressive capacity,
- $N_{dent,c}$ is the characteristic axial compressive capacity of dented member,
- γ_M is resistance factor.

The characteristic axial compressive capacity of dented member can be calculate as follow:

$$N_{dent,c} \begin{cases} (1.0 - 0.28\bar{\lambda}_d^2) \cdot \xi_c \cdot f_y A_0, & \text{for } \bar{\lambda}_d \leq 1.34 \\ \frac{0.9}{\bar{\lambda}_d^2} \cdot \xi_c \cdot f_y A_0, & \text{for } \bar{\lambda}_d > 1.34 \end{cases}, \quad (3.7)$$

where:

- $\bar{\lambda}_d$ is the reduced slenderness of dented member,
- ξ_c is the correction factor for axial resistance of the dented tubular section,
- f_y is the characteristic yield strength,
- A_0 is the cross sectional area.

The reduced slenderness of dented member is calculated as follows:

$$\bar{\lambda}_d = \sqrt{\frac{N_{dent,c}}{N_{E,dent}}} = \sqrt{\frac{\xi_c}{\xi_M}} \cdot \bar{\lambda}_0, \quad (3.8)$$

where:

- $N_{dent,c}$ is the characteristic axial compressive capacity of dented member,
- $N_{E,dent}$ is the Euler buckling strength of a dented tubular member, for buckling in-line with the dent,

- ξ_C is the correction factor for axial resistance of the dented tubular section,
- ξ_M is the correction factor for bending resistance of the dented tubular section,
- $\bar{\lambda}_0$ is the reduced slenderness of undamaged member.

The correction factor for axial resistance is calculated as follow:

$$\xi_C = \exp\left(-0.08 \frac{\delta}{t}\right) \text{ for } \frac{\delta}{t} < 10, \quad (3.9)$$

where:

- δ is the dent depth,
- t is the wall thickness.

The correction factor for bending resistance calculated as follow:

$$\xi_M = \exp\left(-0.06 \frac{\delta}{t}\right) \text{ for } \frac{\delta}{t} < 10, \quad (3.10)$$

where:

- δ is the dent depth,
- t is the wall thickness.

The dent depth calculated as follow:

$$\bar{\delta} = \frac{1}{2} \cdot \left(1 - \cos \pi \frac{A_{crack}}{A}\right) \cdot D, \quad (3.11)$$

where:

- $\bar{\delta}$ is the equivalent dent depth,
- D is the tube diameter,
- A_{crack} is the crack area,
- A is the full cross section area.

As mentioned in chapter 2, the column can have a deviation in the form of an eccentric load. An eccentric load applies to bend the column and the following formula in NORSOK N-004 [8] calculates the bending effect:

$$M_{sd} \leq M_{dent,Rd} = \begin{cases} \xi_M \cdot M_{Rd}, & \text{if the dented area acts in compression} \\ M_{Rd}, & \text{otherwise} \end{cases}, \quad (3.12)$$

where:

- M_{Sd} is the design bending moment,
- $M_{dent,Rd}$ is the design bending capacity of dented section,
- M_{Rd} is the design capacity of undamaged section,
- ξ_M is the correction factor for bending resistance of the dented tubular section, see equation (3.10) in this thesis.

The design bending capacity of undamaged sections is calculated as follow:

$$M_{Rd} = \frac{f_m W}{\gamma_M}, \quad (3.13)$$

where:

- f_m is the characteristic bending strength,
- W is the elastic section modulus,
- γ_M is the material factor.

The characteristic bending strength is calculated as follow:

$$f_m = \begin{cases} \frac{Z}{W} f_y, & \text{for } \frac{f_y D}{Et} \leq 0.0517 \\ \left(1.13 - 2.58 \left(\frac{f_y D}{Et} \right) \left(\frac{Z}{W} \right) \right) f_y, & \text{for } 0.0517 < \frac{f_y D}{Et} \leq 0.1034, \\ \left(0.94 - 0.76 \left(\frac{f_y D}{Et} \right) \left(\frac{Z}{W} \right) \right) f_y, & \text{for } 0.1034 < \frac{f_y D}{Et} \leq 120 \frac{f_y}{E} \end{cases} \quad (3.14)$$

where:

- Z is the plastic section modulus,
- W is the elastic section modulus,
- f_y is the characteristic yield strength,
- D is the outside diameter,
- E is the Young's modulus,
- t is the wall thickness.

The elastic section modulus is calculated as follow:

$$\frac{\pi [D^4 - (D - 2t)^4]}{32 D}, \quad (3.15)$$

where:

D is the outside diameter,

t is the wall thickness.

The plastic section modulus is calculated as follow:

$$\frac{1}{6} [D^3 - (D_{2t})^3], \quad (3.16)$$

where:

D is the outside diameter,

t is the wall thickness.

The design bending capacity of damaged sections is calculated as follow:

$$M_{Sd} \leq M_{dent,Rd} = \begin{cases} \xi_M \cdot M_{Rd}, & \text{if dented area act in compression} \\ M_{Rd}, & \text{otherwise} \end{cases}$$

When bending affects the tubular element it's because of an eccentric load, therefore a combination of both axial and bending should be calculated. Following equations in NORSOK N-004 [8] should be used:

$$\frac{N_{Sd}}{N_{dent,c,Rd}} + \sqrt{\left(\frac{N_{Sd} \Delta y_2 + C_{m1} M_{1,Sd}}{\left(1 - \frac{N_{Sd}}{N_{E,dent}}\right) M_{dent,Rd}} \right)^\alpha + \left(\frac{N_{Sd} \Delta y_1 + C_{m2} M_{2,Sd}}{\left(1 - \frac{N_{Sd}}{N_E}\right) M_{Rd}} \right)^2} \leq 1, \quad (3.17)$$

where:

α is the exponent in stability equation for dented tubular members

$$\alpha = 2 - 3 \frac{\delta}{D},$$

N_{Sd} is the design axial force on the dented section,

$M_{1,Sd}$ is the design bending moment about an axis parallel to the dent,

$M_{2,Sd}$ is the design bending moment about an axis perpendicular to the dent,

$N_{dent,c,Rd}$ is the

$N_{E,dent}$ is the Euler buckling strength of the dented section, for buckling in-line

$$\text{with the dent} = N_{E,dent} = \pi^2 \frac{EI_{dent}}{(kl)^2},$$

k	is the effective length factor,
I_{dent}	is the moment of inertia of the dented cross-section, which may be calculated as: $\xi_M I$,
I	is the moment of inertia of undamaged section,
Δy_1	is the member out-of-straightness perpendicular to the dent,
Δy_2	is the member out-of-straightness in-line with the dent,
C_{m1}, C_{m2}	is the moment reduction factor,

4 Numerical model

4.1 Introduction

There are several finite element programs for creating a numerical model and performing a non-linear buckling analysis. Abaqus is one of them and has been used in this thesis. DNVGL-RP-C208 [9] includes recommendations for performing a non-linear analysis and chapter 4 in DNVGL-RP-C208 describes the requirements. Based on the experimental work the following properties were taken into consideration and implemented in the numerical model: material geometry, elastic and plastic stress and strain, initial geometric imperfection, axial compression load. Three different types of analysis are created, one for fitting the boundary conditions in the test machine and two to match the “physical” buckling shape. The elements types of the columns is a 4-node general-purpose shell element (S4R) that uses reduced integration with hourglass control [10] which is used in the mesh configuration. A non-linear analysis procedure can be divided into the following processes: pre-processing, processing, and post-processing.

Abaqus use consistent units which means that a unit system must be in place. This requires a bit of research before starting modelling.

4.2 Methodology

For a non-linear buckling analysis, some important things must be in place, and suitable software is necessary. The model needs properties such as geometry, mesh, material model, boundary conditions, and load. Then select an appropriate buckling analysis to find the critical buckling load with the belonging buckling shape and implement this in the non-linear analysis to find the axial capacity.

An example of how to perform a buckling analysis is example 8.5 in DNVGL-RP-C208 [9] and contains six steps. These six steps will be gone through:

1. Prepare model: The model needs some preparations such as material properties, geometry, boundary conditions, etc. In structures, it's commonly using steel, and it's a lot of different steel type which affect the material behaviour. The application of the material decides what steel type should be used and is sufficient for the usage. If experimental work is relevant for the case, then the boundary conditions should be the same. Constrains with a reference point in the middle can be used to apply the boundary conditions. A load must be applied. The element type influences the mesh type, and for a tubular element, a 4-noded shell element (S4R) can be used.
2. Determine relevant buckling modes: An eigenvalue analysis can be used to find the different buckling modes and the appropriated critical load. In this step, the goal is to determine the relevant buckling mode.
3. Select object for calibration and prepare model: Models with complicated geometry exist, and calibration can be necessary. The boundary condition, load, mesh, element

type, etc. remain the same. In example 8.5 in DNVGL-RP-C208 [9], a conical transition turns into a cylinder as the calibrated model.

4. Determine the appropriate buckling mode for the calibrated object: The calibrated model has different buckling modes than the original model and is found with an eigenvalue analysis. A comparison between the buckling modes found for the original model and the calibrated is performed. The buckling mode with a similar pattern to the selected buckling mode for the original model is selected as the appropriate buckling mode.
5. Determine magnitude of the equivalent imperfection: The selected buckling mode is implemented in the non-linear analysis, and the model properties used in the eigenvalue analysis remains the same in the non-linear analysis. A buckling capacity calculation performed with formulas in Norsok N-004 [8] is used to determine the magnitude of imperfection. The magnitude of imperfection in the non-linear analysis is scaled, so the axial capacity matches the Norsok N-004 [8] calculations.
6. Perform non-linear analysis of the model with imperfections: The magnitude of imperfection found in step 5 is implemented in the non-linear analysis of the original model then the analysis is performed. The buckling capacity of the model is now found, and the result can be presented as a load-displacement plot.

4.3 Analysis procedure – pre-processing

The pre-processing part of the analysis procedure is where all properties related to the model is performed. In this section, the models used in the non-linear finite element analysis will be described. The model properties such as geometry, mesh, material modelling, boundary conditions and load applications will be described separately.

4.3.1 Software

Two well-known finite element programs are Abaqus and Ansys, and both programs use the finite element method for solving problems. The non-linear behaviour must be considered in the selection of suitable software.

4.3.2 Geometry

Four models have been created and the different geometric properties are described in Table 4-1, three with cracks and one reference model without any defects. The reference model is an undamaged column and the three others have different crack sizes. The crack size is presented in percent of the circumference. There are added holes to the ends of the cracks, Figure 4-2 illustrates this. The samples names contain of some of the geometric properties such as diameter, thickness, hole size and

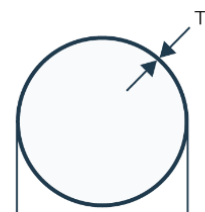


Figure 4-1: Samples cross-section [13].

crack size. For example, 70-2.9-4-88 have a diameter of 70 mm, a thickness of 2.9 mm, holes sizes of 4 mm and a remaining circumference of 88%.

Table 4-1: Geometry properties.

Sample	Diameter	Length	Thickness	Crack size	Hole size
70-2.9-4-100	70 mm	1500 mm	2.9 mm	-	-
70-2.9-4-88	70 mm	1500 mm	2.9 mm	12 %	4 mm
70-2.9-4-76.5	70 mm	1500 mm	2.9 mm	23,5 %	4 mm
70-2.9-4-61.5	70 mm	1500 mm	2.9 mm	38,5%	4 mm

The test setup and how the crack is defined is presented in Figure 4-2. In addition to this, some measurements are added to the figure to show the placement of the crack. Figure 4-2: Samples test setup and crack definition.

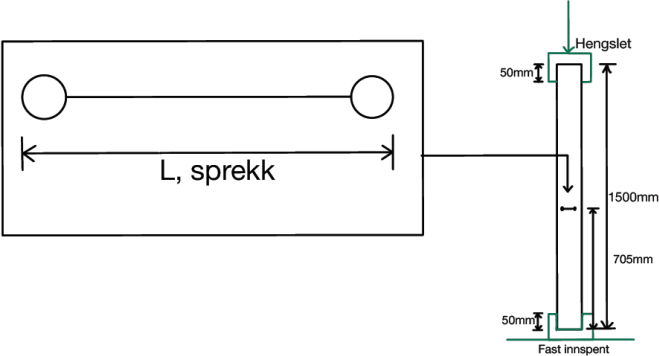


Figure 4-2: Samples test setup and crack definition.

The four different models without any measurement are shown in Figure 4-3 to Figure 4-4.

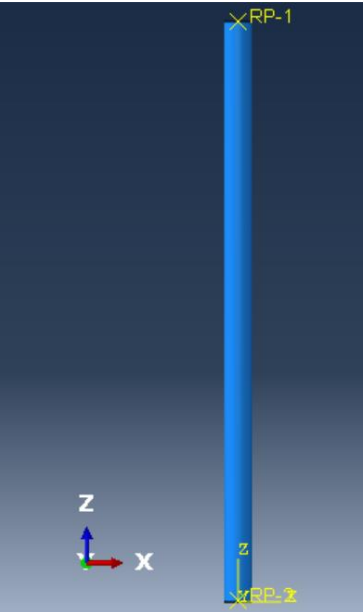


Figure 4-3: Reference model.

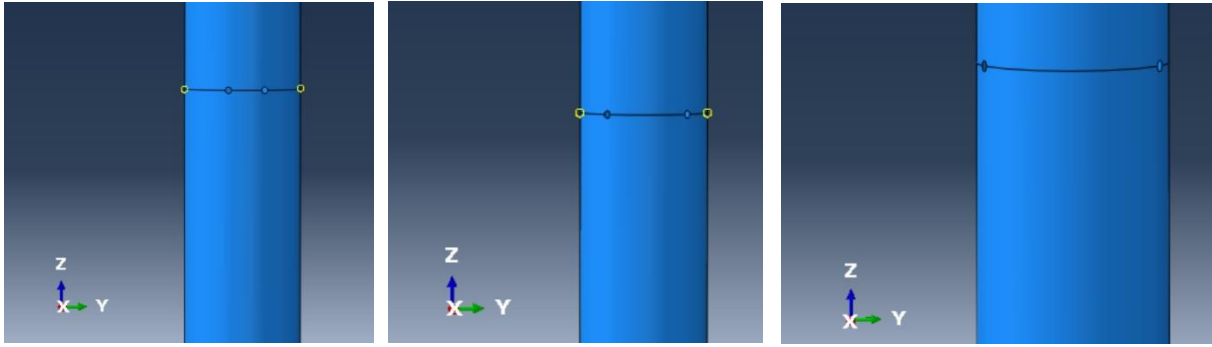


Figure 4-4: 12% crack (left), 23,5% crack (middle) and 38,5% crack (right).

4.3.3 Mesh

The completion time for the analysis would be very long if the whole model had the same mesh density, therefore local seeds are introduced to the model for creating a finer mesh around the crack and holes. This is for focusing on a specific area. The sizes of the global seeds are 3 mm and the local seeds are 0.25 mm around the holes and 0.75 on the crack (the “crack line” between the holes). Since the tubular elements are modelled as a shell, the element type used in the mesh configuration is a 4-node general-purpose shell element (S4R). The column can be exposed to large deformations and large strains, and this element type is capable to handle this.

Figure 4-5 shows the reference model meshed with global seeds of 3 mm.

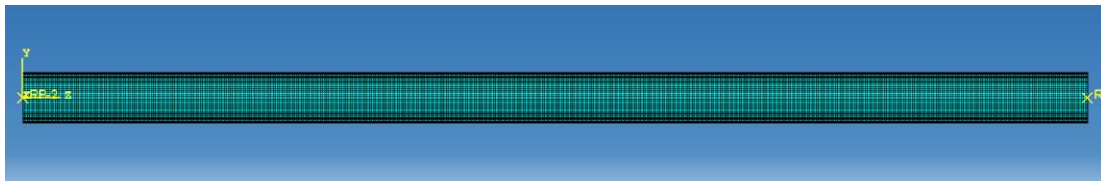


Figure 4-5: Meshed tubular element.

In Figure 4-6, there is created local seeds around the crack and the holes. The global seeds size of 0.25 is the same as for the reference model, and the local seeds have the size of 0.25 mm around the holes and 0.75 mm at the crack line.

Mesh refinement is necessary to see what the results converge to. The results from different mesh sizes are compared to see what the results converge to. When the differences are low, the mesh refinement is done. All the numerical models have been through mesh refinement.

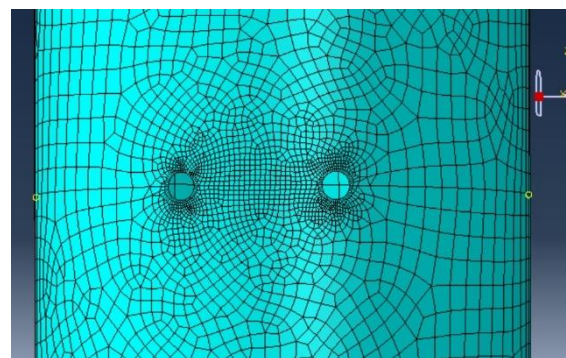


Figure 4-6: Local seeds introduced in the numerical model with 12% crack.

4.3.4 Material modelling

The material properties are important to look at because different steel types have different behaviours. A stress-strain plot is used to describe the stress development and the elastic and plastic area can be defined here. From the elastic region, Young's modulus can be found. The value of Young's modulus and yield stress is obtained from the experimental work performed by Simen Riise [11]. In Table 4-2 the material properties such as Young's modulus, Poisson's Ratio and yield stress is summarized.

Table 4-2: Material properties.

Young's Modulus (E):	150 000 MPa
Poisson's Ratio (ν):	0.3
Yield stress (σ _Y):	370 MPa

In a non-linear analysis the plasticity is also used, and the yield stress-strain relation must be defined. The stresses found from experimental work have a so-called engineering stress-strain relation, and the true stress-strain relation is required in the non-linear analysis. There are formulas in DNVGL-RP-C208 [9] that can be used to convert from engineering stress-strain to true stress-strain. In Table 4-3 the converting formulas presented in DNVGL-RP-C208 are presented.

Table 4-3: Formula for converting from "engineering" stress-strain to "true" stress-strain. Bottom left = formula (6), bottom right = formula (7). Reference [9].

Engineering stress → true stress	Engineering strain → true strain
$\sigma_{\text{true}} = \sigma_{\text{eng}}(1 + \epsilon_{\text{eng}})$	$\epsilon_{\text{true}} = \ln(1 + \epsilon_{\text{eng}})$

The true-strains values are summarized in Table 4-4, and they are implemented in the non-linear analysis.

Table 4-4: "True" stress and true "strain" after using eq. 6 and eq7 in DNV-RP-C208 [9].

Yield stress (MPa)	Plastic strain
370	0
371,48	0,004
377,40	0,0198
444,00	0,1823

Three components can be used for describing the material model's plasticity:

- Yield surface: Von Mises yield criteria is used for making a yield surface plot. This shows when the plastic strains are generated.

- Isotropic hardening: A new yield surface can be created when the materials plastic strains grow, and the isotropic hardening presents these changes.
- Flow rule: The strain increment and the stress increment having a relation between each other.

Isotropic hardening has been used in the numerical model. The yield surface for the numerical model with steel S235 and the isotropic hardening are presented in Figure 4-7.

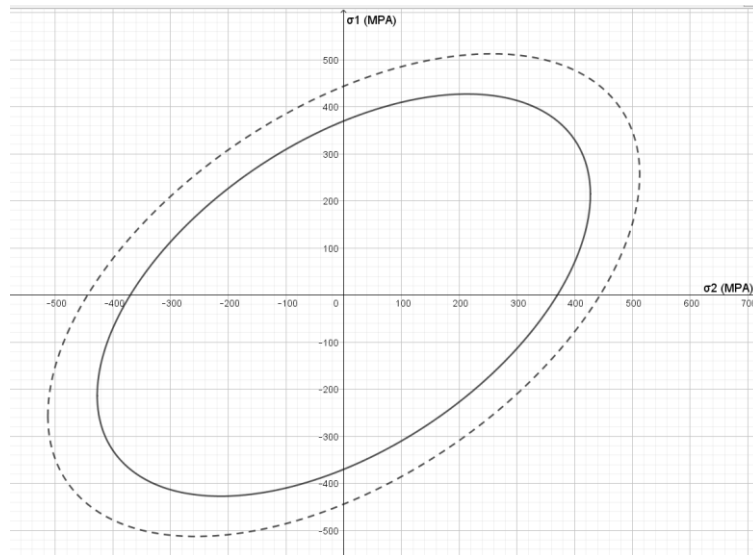


Figure 4-7: Yields surface and isotropic hardening.

4.3.5 Boundary conditions

There have been used three different types of boundary conditions for the numerical models and they are divided into three cases:

- Case 1: bottom is fixed, and the top is hinged.
- Case 2: bottom is fixed, and the top is fixed.
- Case 3: bottom is pinned, and the top is pinned.

Following degrees of freedom are restrained for case 1: all at the bottom, U1 and U2 at top. Following degrees of freedom are restrained for case 2: all at the bottom and top.

Following degrees of freedom are restrained for case 3: U1, U2, U3, UR3 at the bottom, and U1, U2, UR3 at the top.

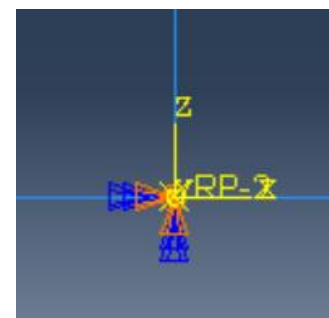


Figure 4-8: Boundary conditions case 1 (fixed-hinged).

4.3.6 Load application

Two types of loads are used in the numerical models. There has been used a concentrated force as the load in the linear buckling analysis and the magnitude of this has been set to 1. This load is applied to the centre at the top of the columns. An eigenvalue is found which refer to the critical buckling load. There have not been applied a real load in the non-linear analysis, but a displacement has been applied at the top centre. This displacement acts like a compression load.

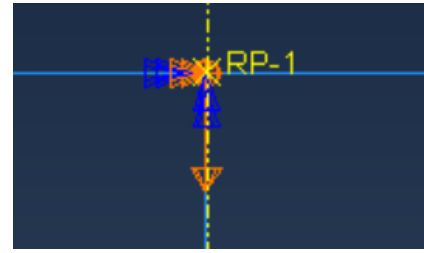


Figure 4-9: Load applied at the top of the models.

4.4 Analysis procedure – processing

In the pre-processing, the model was created and now it's time for performing a buckling analysis as the processing part. All the necessary inputs in the buckling analysis will be described in this section. In addition, the non-linear analysis will be described shortly.

4.4.1 Analysis method

The linear buckling analysis is used to determine the possible buckling modes of a perfect column. In Abaqus, the buckling analysis can be an eigenvalue-based analysis which means that the buckling mode and the appropriated eigenvalue are found, and this type of analysis is used for the numerical models.

There are two types of eigensolvers to choose, either the subspace or the Lanczos and both extract the different eigenmodes. How many eigenmodes which is desirable and how many of them are of interest must be defined. There are also possible to specify how many *vectors used per iteration* but Abaqus gives a suggestion here, and the last thing to specify is the *maximum number of iterations*, this can be a random number, but a high number is recommended.

The linear buckling analysis gives different eigenmodes with different buckling shapes. It was desirable to have a similar buckling shape as in the experimental work, therefore were the chosen buckling modes either mode one or mode two and both modes have the same buckling shapes, but they are buckling about either x- or y-axis. Since the holes and crack were facing in the x-direction, the mode which buckling about the x-axis was chosen.

The non-linear finite element analysis using the Newton-Raphson method to solve the non-linear problem. The static general analysis in Abaqus can meet on problems in the analysis because of unstable problems. The converge criteria will fail for unstable structures.

4.5 Analysis procedure – post-processing

The post-processing process contains of selecting the relevant buckling mode and implements this into the non-linear analysis, and a scale factor must be defined. The magnitude of the scale factor can either be set to a desired value or it can be set to match a calculated value.

By implementing the buckling shape, the non-linear analysis is told that there is an imperfection in the model.

4.5.1 Imperfections (imperfections shape – magnitude)

The relevant buckling mode from the eigenmode analysis must be determined. Then the non-linear analysis is told that this imperfection shape will occur, and the capacity calculations are based on this shape. The relevant buckling mode in the numerical models was the shape that was most like the buckling shape in the experimental work. The magnitude of this is based on the eccentricity in the experimental work which was between 1.5 mm to 2 mm. Following three scaling factors have been used in the non-linear analysis: 1.5, 1.8 and 2.0. There have been used both negative and scaling factors, the difference is which way the column is buckling. The positive scale factor tells the imperfection shape to buckle the same way as the selected eigenmode and it is the opposite when the scale factor becomes negative.

4.5.2 Postbuckling analysis

There is possible to perform another type of non-linear analysis if it is suspected that there is an unstable response. The “Riks method” can be introduced with the same imperfections described in the previous paragraph. This has not been done for the numerical models, only a few tests to see how the load-displacement plots are changing.

4.6 Results

4.6.1 Fixed-hinged boundary conditions

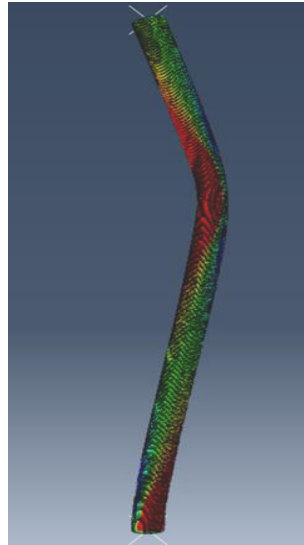


Figure 4-10: Buckling shape of column with fixed-pinned boundary conditions.

The results from the non-linear finite element analysis with fixed-pinned boundary conditions for three different scale factors are summarized in Table 4-5 to Table 4-7.

Table 4-5: Results from non-linear finite element analysis with positive and negative scale factor equal to 1.5. Boundary conditions: fixed-pinned.

Sample	Crack size ¹	Axial capacity, kN	
		$P_{FE,neg}^2$	$P_{FE,pos}^3$
70-2.9-4-100	0	215.08	215.08
70-2.9-4-88	12.0	212.31	215.09
70-2.9-4-76.5	23.5	-(⁴)	214.00
70-2.9-4-61.5	38.5	214.63	-(⁴)

1. Crack size is given in percent of the original circumference, 2. FE,neg = negative scale factor, 3. FE,pos = positive scale factor, 4. Abaqus failed to calculate.

Table 4-6: Results from non-linear finite element analysis with positive and negative scale factor equal to 1.8. Boundary conditions: fixed-pinned.

Sample	Crack size ¹	Axial capacity, kN	
		$P_{FE,neg}^2$	$P_{FE,pos}^3$
70-2.9-4-100	0	207.69	207.69
70-2.9-4-88	12.0	207.43	207.93
70-2.9-4-76.5	23.5	211.24	213.59
70-2.9-4-61.5	38.5	213.32	207.88

1. Crack size is given in percent of the original circumference, 2. FE,neg = negative scale factor, 3. FE,pos = positive scale factor.

Table 4-7: Results from non-linear finite element analysis with positive and negative scale factor equal to 2.0. Boundary conditions: fixed-pinned.

Sample	Crack size ¹	Axial capacity, kN	
		P _{FE,neg} ²	P _{FE,pos} ³
70-2.9-4-100	0	204.13	204.13
70-2.9-4-88	12.0	204.87	207.57
70-2.9-4-76.5	23.5	-(⁴)	-(⁴)
70-2.9-4-61.5	38.5	-(⁴)	-(⁴)

1. Crack size is given in percent of the original circumference, 2. FE,neg = negative imperfection, 3. FE,pos = positive imperfection, 4. Abaqus failed to calculate.

4.6.2 Pinned-pinned boundary conditions

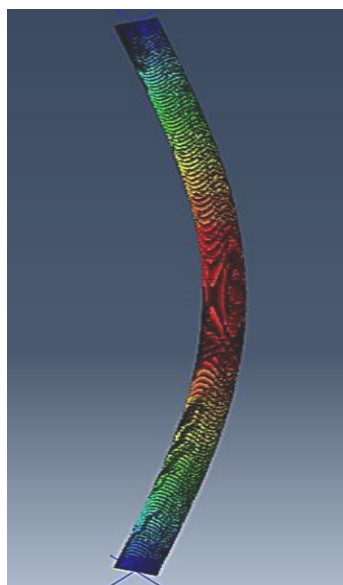


Figure 4-11. Buckling shape of column with pinned-pinned boundary conditions.

The results from the non-linear finite element analysis with pinned-pinned boundary conditions for three different scale factors are summarized in Table 4-8 to Table 4-10.

Table 4-8: Results from non-linear finite element analysis with positive and negative scale factor equal to 1.5. Boundary conditions: pinned-pinned.

Sample	Crack size ¹	Axial capacity, kN	
		P _{FE,neg} ²	P _{FE,pos} ³
70-2.9-4-100	0	184.36	184.36
70-2.9-4-88	12.0	177.21	184.72
70-2.9-4-76.5	23.5	177.50	184.68
70-2.9-4-61.5	38.5	-(⁴)	-(⁴)

1. Crack size is given in percent of the original circumference, 2. FE,neg = negative scale factor, 3. FE,pos = positive scale factor, 4. Abaqus failed to calculate

Table 4-9: Results from non-linear finite element analysis with positive and negative scale factor equal to 1.8. Boundary conditions: pinned-pinned.

Sample	Crack size ¹	Axial capacity, kN	
		P _{FE,neg} ²	P _{FE,pos} ³
70-2.9-4-100	0	_(4)	_(4)
70-2.9-4-88	12.0	172.74	177.76
70-2.9-4-76.5	23.5	_(4)	_(4)
70-2.9-4-61.5	38.5	178.07	171.18

1. Crack size is given in percent of the original circumference, 2. FE,neg = negative scale factor, 3. FE,pos = positive scale factor, 4. Abaqus failed to calculate.

Table 4-10: Results from non-linear finite element analysis with positive and negative scale factor equal to 2.0. Boundary conditions: pinned-pinned.

Sample	Crack size ¹	Axial capacity, kN	
		P _{FE,neg} ²	P _{FE,pos} ³
70-2.9-4-100	0	176.49	176.49
70-2.9-4-88	12.0	164.31	176.70
70-2.9-4-76.5	23.5	170.29	176.46
70-2.9-4-61.5	38.5	_(4)	_(4)

1. Crack size is given in percent of the original circumference, 2. FE,neg = negative scale factor, 3. FE,pos = positive imperfection, 4. Abaqus failed to calculate.

4.6.3 Fixed-fixed boundary conditions

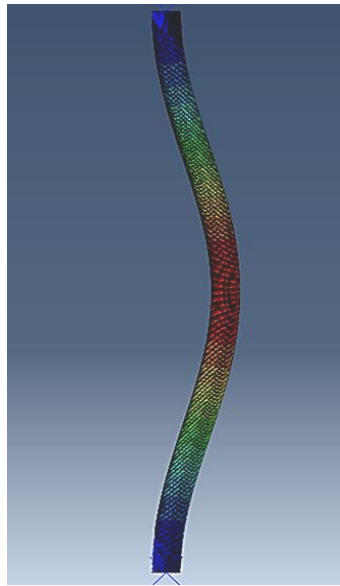


Figure 4-12: Buckling shape of column with pinned-pinned boundary conditions.

The results from the non-linear finite element analysis with fixed-fixed boundary conditions for three different scale factors are summarized in Table 4-11 to Table 4-13.

Table 4-11: Results from non-linear finite element analysis with positive and negative scale factor equal to 1.5. Boundary conditions: fixed-fixed.

Sample	Crack size ¹	Axial capacity, kN	
		$P_{FE,neg}^2$	$P_{FE,pos}^3$
70-2.9-4-100	0	227.00	227.00
70-2.9-4-88	12.0	220.42	227.49
70-2.9-4-76.5	23.5	221.15	227.17
70-2.9-4-61.5	38.5	223.70	225.91

1. Crack size is given in percent of the original circumference, 2. FE,neg = negative imperfection, 3. FE,pos = positive imperfection.

Table 4-12: Results from non-linear finite element analysis with positive and negative scale factor equal to 1.8. Boundary conditions: fixed-fixed.

Sample	Crack size ¹	Axial capacity, kN	
		$P_{FE,neg}^2$	$P_{FE,pos}^3$
70-2.9-4-100	0	225.21	225.21
70-2.9-4-88	12.0	219.51	225.65
70-2.9-4-76.5	23.5	220,09	225.17
70-2.9-4-61.5	38.5	221.54	224.13

1. Crack size is given in percent of the original circumference, 2. FE,neg = negative imperfection, 3. FE,pos = positive imperfection.

Table 4-13: Results from non-linear finite element analysis with positive and negative scale factor equal to 2.0. Boundary conditions: fixed-fixed.

Sample	Crack size ¹	Axial capacity, kN	
		P _{FE,neg} ²	P _{FE,pos} ³
70-2.9-4-100	0	223.95	223.95
70-2.9-4-88	12.0	218.62	225.65
70-2.9-4-76.5	23.5	219.01	224.21
70-2.9-4-61.5	38.5	221.11	222.96

1. Crack size is given in percent of the original circumference, 2. FE,neg = negative imperfection, 3. FE,pos = positive imperfection.

5 Comparison and discussion

5.1 Introduction

The numerical model is modelled and performed based on the description described in the previous chapter. Imperfection and non-linear stress-strain behaviour are included in the model. This chapter presents the result from the non-linear finite element analysis, experimental work, hand calculations according to NORSOK N-004 and comparison and discussion of the results.

5.2 Non-linear finite element method

The magnitude of imperfection influences the axial capacity of a column. There have been performed three non-linear analysis with different magnitude of imperfection, one with fixed-hinged boundary conditions, one with pinned-pinned boundary conditions, and one with pinned-pinned boundary conditions. In all three analyses, the same magnitude of imperfection has been applied to the model. Three different scaling factors has been used. The scaling factors have had both positive and negative values.

5.2.1 Fixed-hinged boundary conditions

The results from the non-linear finite element analysis with fixed-hinged boundary conditions for three different scale factors are summarized in Table 5-1 Table 4-5 to Table 5-3.

In Table 5-1, there is a difference of 1.3 % between the highest and lowest axial capacity. For the positives scaling factors, there is a decrease in the axial capacity of 1 kN which is nothing. There are missing two results in the table, and the reason can be an unstable problem.

Table 5-1: Results from non-linear finite element analysis with positive and negative scale factor equal to 1.5. Boundary conditions: fixed-hinged.

Sample	Crack size ¹	Axial capacity, kN	
		P _{FE,neg} ²	P _{FE,pos} ³
70-2.9-4-100	0	215.08	215.08
70-2.9-4-88	12.0	212.31	215.09
70-2.9-4-76.5	23.5	-(⁴)	214.00
70-2.9-4-61.5	38.5	214.63	-(⁴)

1. Crack size is given in percent of the original circumference, 2. FE,neg = negative scale factor, 3. FE,pos = positive scale factor, 4. Abaqus failed to calculate.

The results with scaling factor of ± 1.8 are summarized in Table 5-2, and there is a difference of 2.8 % between the highest and lowest axial capacity. The highest capacity with a positive scale factor is the damaged column with 23.5 % crack size and the weakest column is the reference column. The two largest crack sizes have higher capacity than the reference column when the scale factor change to minus, and again it's no big differences in the capacity.

Table 5-2: Results from non-linear finite element analysis with positive and negative scale factor equal to 1.8. Boundary conditions: fixed-hinged.

Sample	Crack size ¹	Axial capacity, kN	
		P _{FE,neg} ²	P _{FE,pos} ³
70-2.9-4-100	0	207.69	207.69
70-2.9-4-88	12.0	207.43	207.93
70-2.9-4-76.5	23.5	211.24	213.59
70-2.9-4-61.5	38.5	213.32	207.88

1. Crack size is given in percent of the original circumference, 2. FE,neg = negative scale factor, 3. FE,pos = positive scale factor.

Table 5-3 missing some of the results with a scaling factor of ± 2.0 , this can be because of an unstable problem again. The difference between the highest and lowest axial capacity for the available results is 1.7 % which are nothing. In common, the capacity are increasing when a crack occurs.

Table 5-3: Results from non-linear finite element analysis with positive and negative scale factor equal to 2.0. Boundary conditions: fixed-hinged.

Sample	Crack size ¹	Axial capacity, kN	
		P _{FE,neg} ²	P _{FE,pos} ³
70-2.9-4-100	0	204.13	204.13
70-2.9-4-88	12.0	204.87	207.57
70-2.9-4-76.5	23.5	-(⁴)	-(⁴)
70-2.9-4-61.5	38.5	-(⁴)	-(⁴)

1. Crack size is given in percent of the original circumference, 2. FE,neg = negative imperfection, 3. FE,pos = positive imperfection, 4. Abaqus failed to calculate.

To summarize Table 5-1 to Table 5-3, there are small differences between the results for the respective scaling factors, they vary from 1.3 % to 2.8 %. The highest axial capacity is found for the column with the lowest magnitude of imperfection (lowest scale factor). Some results are missing, and unstable problems can be the reason.

5.2.2 Pinned-pinned boundary conditions

The results obtained from the non-linear analysis with pinned-pinned boundary conditions are presented in Table 5-4 to Table 5-6. Three different scale factors (1.5, 1.8, 2.0) have been implemented in the non-linear analysis.

In Table 5-4 the axial capacity obtained from the non-linear analysis with a scale factor of 1.5 and pinned-pinned boundary conditions is presented. Some results missing for the last sample, and this can be because of an unstable problem. Another thing to notice is the small change in the axial capacity for the positive scale factor. The total difference between the highest and lowest axial capacity is 4.1 %.

Table 5-4: Results from non-linear finite element analysis with positive and negative scale factor equal to 1.5. Boundary conditions: pinned-pinned.

Sample	Crack size ¹	Axial capacity, kN	
		P _{FE,neg} ³	P _{FE,pos} ⁴
70-2.9-4-100	0	184.36	184.36
70-2.9-4-88	12.0	177.21	184.72
70-2.9-4-76.5	23.5	177.50	184.68
70-2.9-4-61.5	38.5	-(2)	-(2)

1. Crack size is given in percent of the original circumference, 2. Abaqus failed to calculate. 3. FE,neg = negative imperfection, 4. FE,pos = positive imperfection.

The axial capacity with scale factor 1.8 is presented in Table 5-5, and two samples are missing data. An interesting thing about the negative scale factor is when the crack size increases, the capacity also increases. It is the opposite for the positive scale factor, the capacity decreases. It is impossible to say the two patterns remain the same when data for the missing results are found. The difference between the highest axial capacity and lowest capacity is 4 %.

Table 5-5: Results from non-linear finite element analysis with positive and negative scale factor equal to 1.8. Boundary conditions: pinned-pinned.

Sample	Crack size ¹	Axial capacity, kN	
		P _{FE,neg} ³	P _{FE,pos} ⁴
70-2.9-4-100	0	-(2)	-(2)
70-2.9-4-88	12.0	172.74	177.76
70-2.9-4-76.5	23.5	-(2)	-(2)
70-2.9-4-61.5	38.5	178.07	171.18

1. Crack size is given in percent of the original circumference, 2. Abaqus failed to calculate. 3. FE,neg = negative imperfection, 4. FE,pos = positive imperfection.

In Table 5-6 the axial capacity with scale factor 2 is presented. There are missing data for the largest crack, and this can be because of an unstable analysis. The axial capacity differences are small when the positive scale factor is applied. When it comes to the negative scale factor, the reference model has a higher capacity than the two cracked ones, but the capacity is increasing when the crack becomes bigger. There is a difference of 7.5 % when the highest and lowest axial capacity is compared.

Table 5-6: Results from non-linear finite element analysis with positive and negative scale factor equal to 2.0. Boundary conditions: pinned-pinned.

Sample	Crack size ¹	Axial capacity, kN	
		P _{FE,neg} ³	P _{FE,pos} ⁴
70-2.9-4-100	0	176.49	176.49
70-2.9-4-88	12.0	164.31	176.70
70-2.9-4-76.5	23.5	170.29	176.46
70-2.9-4-61.5	38.5	-(²)	-(²)

1. Crack size is given in percent of the original circumference, 2. Abaqus failed to calculate. 3. FE,neg = negative imperfection, 4. FE,pos = positive imperfection.

To summarize the results in Table 5-4 to Table 5-6, some results are missing from the non-linear analysis performed in Abaqus. The difference in the axial capacity is in the range of 4% to 7.5 %. The axial capacity decreases when the imperfection magnitude increase. A reason for the missing results from the non-linear analysis can be because of unstable problems.

5.2.3 Fixed-fixed boundary conditions

The results obtained from the non-linear analysis with fixed-fixed boundary conditions are represented in Table 5-7 to Table 5-9. The same three scale factors that were used for the two previous cases are implemented in the non-linear analysis. Unlike the previous boundary conditions, all demanded values are found. This gives a good picture of how the axial capacity changes with different scale factors.

In Table 5-7 the axial capacity obtained from the non-linear analysis with scale factor 1.5 is presented. All samples have results for both negative and positive scale factors. There is a difference of 3 % between the highest and lowest capacity. The reference model has a higher capacity than the cracked samples when the scale factor is positive, but the axial capacity is increasing when the crack gets bigger. There is a difference of 0.7 % with a positive scale factor.

Table 5-7: Results from non-linear finite element analysis with positive and negative scale factor equal to 1.5. Boundary conditions: fixed-fixed.

Sample	Crack size ¹	Axial capacity, kN	
		P _{FE,neg} ²	P _{FE,pos} ³
70-2.9-4-100	0	227.00	227.00
70-2.9-4-88	12.0	220.42	227.49
70-2.9-4-76.5	23.5	221.15	227.17
70-2.9-4-61.5	38.5	223.70	225.91

1. Crack size is given in percent of the original circumference, 2. FE,neg = negative imperfection, 3. FE,pos = positive imperfection.

The axial capacity obtained from the non-linear analysis with scale factor 1.8 is presented in Table 5-8. The difference in axial capacity is 2.8 % when the highest axial capacity is compared with the lowest. There is a difference of 0.7 % when the axial capacity for the positive scale factor is compared.

Table 5-8: Results from non-linear finite element analysis with positive and negative scale factor equal to 1.8. Boundary conditions: fixed-fixed.

Sample	Crack size ¹	Axial capacity, kN	
		P _{FE,neg} ²	P _{FE,pos} ³
70-2.9-4-100	0	225.21	225.21
70-2.9-4-88	12.0	219.51	225.65
70-2.9-4-76.5	23.5	220,09	225.17
70-2.9-4-61.5	38.5	221.54	224.13

1. Crack size is given in percent of the original circumference, 2. FE,neg = negative imperfection, 3. FE,pos = positive imperfection.

In Table 5-9 the axial capacity obtained from the non-linear analysis with scale factor 2.0 is presented. There are 3.2 % differences in the highest and lowest axial capacity. Two patterns can describe the development of the axial capacity. When the scale factor is set a to positive value, the axial capacity decreases when the crack gets bigger. It is the opposite for the negative scale factor, the crack is increasing, and the axial capacity is also increasing.

Table 5-9: Results from non-linear finite element analysis with positive and negative scale factor equal to 2.0. Boundary conditions: fixed-fixed.

Sample	Crack size ¹	Axial capacity, kN	
		P _{FE,neg} ²	P _{FE,pos} ³
70-2.9-4-100	0	223.95	223.95
70-2.9-4-88	12.0	218.62	225.65
70-2.9-4-76.5	23.5	219.01	224.21
70-2.9-4-61.5	38.5	221.11	222.96

1. Crack size is given in percent of the original circumference, 2. FE,neg = negative imperfection, 3. FE,pos = positive imperfection.

To summarize the results in Table 5-7 to Table 5-9, all samples are represented for the three different scale factors. The axial capacity is decreased when the magnitude of the scale factor increases. The difference of the axial capacity with the respective scale factor is in the range of 2.8 % to 3.2 % that shows a good match.

5.3 Experimental results

The axial capacity obtained from the experimental work and non-linear finite element analysis is presented in Table 5-10 to Table 5-12. The three different cases, fixed-hinged boundary conditions, pinned-pinned boundary conditions, fixed-fixed boundary conditions are compared with the experimental work. The highest axial capacity from the non-linear analysis is used in the comparison which is with a scale factor of minus 1.5.

In Table 5-10 the results from the experimental work and the first non-linear case (fixed-hinged boundary conditions) are compared. The results show that there is a good match between the calculated axial capacities.

Table 5-10: Experimental [11] and non-linear finite element results (fixed-hinged) and the ratio between the results.

Sample	Crack size ¹	Axial capacity, kN		Ratio
		P _{Exp}	P _{FE,ref} ⁴	
70-2.9-4-100-1	0	208.95	215.13	0.97
70-2.9-4-88-1-UD ²	12.0	203.75	212.31	0.96
70-2.9-4-88-2	12.0	200.61	212.31	0.95
70-2.9-4-88-3-OD ³	12.0	206.49	212.31	0.97
70-2.9-4-76.5-1	23.5	204.22	211.24 ⁽⁵⁾	0.97
70-2.9-4-76.5-2-OD ³	23.5	199.30	211.24 ⁽⁵⁾	0.94
70-2.9-4-61.5-1	38.5	210.70	214.63	0.98
70-2.9-4-61.5-2-OD ³	38.5	200.67	214.63	0.93

1. Crack size is given in percent of the original circumference, 2. UD = sample was putted wrong way in the test machine, 3. OD = the sample was rotated 180° around z- axis, 4. FE,ref = fixed-hinged finite element model, 5. Abaqus failed to calculated for scale factor -1,5, therefore the scale factor has been set to -1.7.

The fixed-fixed boundary conditions are compared with the experimental work in Table 5-11. The boundary conditions are stiffer than the boundary conditions which was represented in the experimental work, therefore the axial capacity should be higher than the experimental work.

Table 5-11: Experimental [11] and non-linear finite element results (fixed-fixed) and the ratio between the results.

Sample	Crack size ¹	Axial capacity, kN		Ratio
		P _{Exp}	P _{FE,fixed} ⁴	
70-2.9-4-100-1	0	208.95	227.00	0.92
70-2.9-4-88-1-UD ²	12.0	203.75	220.42	0.92
70-2.9-4-88-2	12.0	200.61	220.42	0.91
70-2.9-4-88-3-OD ³	12.0	206.49	227.49	0.91
70-2.9-4-76.5-1	23.5	204.22	221.15	0.92
70-2.9-4-76.5-2-OD ³	23.5	199.30	227.17	0.88
70-2.9-4-61.5-1	38.5	210.70	223.70	0.94
70-2.9-4-61.5-2-OD ³	38.5	200.67	225.91	0.89

1. Crack size is given in percent of the original circumference, 2. UD = sample was putted wrong way in the test machine, 3. OD = the sample was rotated 180° around z- axis, 4. FE,ref = fixed-fixed finite element model.

In Table 5-12, the results from the non-linear analysis with pinned-pinned are compared with the experimental work. The boundary conditions in the non-linear analysis are weaker than the boundary conditions in the experimental work, therefore the axial capacity should be lower than the experimental work.

Table 5-12: Experimental [11] and non-linear finite element results (pinned-pinned) and the ratio between the results.

Sample	Crack size ¹	Axial capacity, kN		Ratio
		P _{Exp}	P _{FE,pinned} ⁴	
70-2.9-4-100-1	0	208.95	184.36	1.13
70-2.9-4-88-1-UD ²	12.0	203.75	177.21	1.15
70-2.9-4-88-2	12.0	200.61	177.21	1.13
70-2.9-4-88-3-OD ³	12.0	206.49	184.72	1.12
70-2.9-4-76.5-1	23.5	204.22	177.50	1.15
70-2.9-4-76.5-2-OD ³	23.5	199.30	184.68	1.08
70-2.9-4-61.5-1	38.5	210.70	178.07	1.18
70-2.9-4-61.5-2-OD ³	38.5	200.67	171.18	1.17

1. Crack size is given in percent of the original circumference, 2. UD = sample was putted wrong way in the test machine, 3. OD = the sample was rotated 180° around z- axis, 4. FE,ref = pinned-pinned finite element model.

To summarize the results in Table 5-10 to Table 5-12, three different boundary conditions have been used in the comparison. The first case (fixed-hinged) show a good match in the results, and the differences are in the range of 2 % to 7 %. The other two cases (fixed-fixed and pinned-pinned) shows higher and lower axial capacity in the comparison. There is missing some data from the non-linear analysis in the comparison of the first case. The reason for this can be because of an unstable problem and the analysis fail.

5.4 NORSOK N-004

In Table 5-13 the hand calculations performed with NORSOK N-004 formulas are compared with the experimental work. In addition, the three different non-linear analysis has also been compared with the NORSOK N-004 results and are found in Table 5-14 to Table 5-16. There have been used three different effective length factors (k) in the hand calculations and they are 0.5, 0.7 and 1.0. These factors are based on figure 7.112 in Handbook of Offshore Engineering [12]. Appendix A shows the hand calculations performed by NORSOK N-004.

The comparison between the experimental results and NORSOK N-004 are summarized in Table 5-13. There is a difference of 13 % between the axial capacity for the undamaged column.

Table 5-13: Results from NORSOK N-004 and the experimental work [11] and ratio between the results.

Sample	Crack size ¹	Axial capacity, kN		
		P_{NORSOK} ($k = 0.7$)	P_{Exp}	Ratio
70-2.9-4-100-1	0	181.27	208.95	0.87
70-2.9-4-88-1-UD ²	12.0	168.77	203.75	0.83
70-2.9-4-88-2	12.0	168.77	200.61	0.84
70-2.9-4-88-3-OD ³	12.0	168.77	206.49	0.82
70-2.9-4-76.5-1	23.5	138.55	204.22	0.68
70-2.9-4-76.5-2-OD ³	23.5	138.55	199.30	0.70
70-2.9-4-61.5-1	38.5	88.61	210.70	0.42
70-2.9-4-61.5-2-OD ³	38.5	88.61	200.67	0.44

1. Crack size is given in percent of the original circumference, 2. UD = sample was putted wrong way in the test machine, 3. OD = the sample was rotated 180° around z- axis. The effective length factor (k) is set to 0.7 for fixed-hinged.

Three different boundary conditions cases performed by non-linear analysis and NORSOK N-004 calculations are summarized in Table 5-14 to Table 5-16. There are no huge differences in the ratio when the ratio from the different cases are compared with each other.

Table 5-14: Results from NORSOK N-004 and non-linear finite element analysis (fixed-hinged) and ratio between the results.

Sample	Crack size ¹	Axial capacity, kN		
		P _{NORSOK} (k = 0.7)	P _{FE,ref} ⁴	Ratio
70-2.9-4-100-1	0	181.27	215.13	0.84
70-2.9-4-88-1-UD ²	12.0	168.77	212.31	0.79
70-2.9-4-88-2	12.0	168.77	212.31	0.79
70-2.9-4-88-3-OD ³	12.0	168.77	212.31	0.79
70-2.9-4-76.5-1	23.5	138.55	211.24 ⁽⁵⁾	0.66
70-2.9-4-76.5-2-OD ³	23.5	138.55	211.24 ⁽⁵⁾	0.66
70-2.9-4-61.5-1	38.5	88.61	214.63	0.41
70-2.9-4-61.5-2-OD ³	38.5	88.61	214.63	0.41

1. Crack size is given in percent of the original circumference, 2. UD = sample was putted wrong way in the test machine, 3. OD = the sample was rotated 180° around z- axis, 4. FE,ref = fixed-hinged finite element model, 5. Abaqus failed to calculate for scale factor 1.5, value from 1.7 are used instead. The effective length factor (k) is set to 0.7 for fixed-hinged.

Table 5-15: Results from NORSOK N-004 and non-linear finite element analysis (pinned-pinned) and ratio between the results.

Sample	Crack size ¹	Axial capacity, kN		
		P _{NORSOK} (k = 1)	P _{FE,pinned} ⁴	Ratio
70-2.9-4-100-1	0	155.10	184.36	0.84
70-2.9-4-88-1-UD ²	12.0	145.14	177.21	0.82
70-2.9-4-88-2	12.0	145.14	177.21	0.82
70-2.9-4-88-3-OD ³	12.0	145.14	184.72	0.79
70-2.9-4-76.5-1	23.5	120.76	177.50	0.68
70-2.9-4-76.5-2-OD ³	23.5	120.76	184.68	0.65
70-2.9-4-61.5-1	38.5	79.17	178.07	0.44
70-2.9-4-61.5-2-OD ³	38.5	79.17	171.18	0.46

1. Crack size is given in percent of the original circumference, 2. UD = sample was putted wrong way in the test machine, 3. OD = the sample was rotated 180° around z- axis, 4. FE,pinned = pinned-pinned finite element model. The effective length factor (k) is set to 0.5 for fixed-fixed.

Table 5-16: Results from NORSOK N-004 and non-linear finite element analysis (fixed-fixed) and ratio between the results.

Sample	Crack size ¹	Axial capacity, kN		
		P _{NORSOK} (k = 0.5)	P _{FE, fixed} ⁴	Ratio
70-2.9-4-100-1	0	193.75	227.00	0.85
70-2.9-4-88-1-UD ²	12.0	180.02	220.42	0.82
70-2.9-4-88-2	12.0	180.02	220.42	0.82
70-2.9-4-88-3-OD ³	12.0	180.02	227.49	0.80
70-2.9-4-76.5-1	23.5	147.01	221.15	0.67
70-2.9-4-76.5-2-OD ³	23.5	147.01	227.17	0.65
70-2.9-4-61.5-1	38.5	93.11	223.70	0.42
70-2.9-4-61.5-2-OD ³	38.5	93.11	225.91	0.41

1. Crack size is given in percent of the original circumference, 2. UD = sample was putted wrong way in the test machine, 3. OD = the sample was rotated 180° around z- axis, 4. FE, fixed = fixed-hinged finite element model. The effective length factor (k) is set to 1 for pinned-pinned.

To summarize the results in Table 5-13 to Table 5-16, both experimental results and non-linear finite element analysis are compared with the hand calculations performed with NORSOK N-004. In common for the two first tables, the axial capacity comparison has a difference of 1 % to 5 %. This means that there is a good match between the results. Another good thing is that the axial capacity found in the hand calculations are lower than the experimental work. This shows that there is implemented safety factor in the formulas to be on the safe side when calculate structural elements.

Another thing to mention is the differences in the calculations of the cracked samples. There are huge differences in the results when the crack size becomes big. In the non-linear analysis, there is implemented a non-linear behavior. This are not done in the hand calculations and that should be done, the problem had been to complex to solve by hand.

6 Conclusion and further work

6.1 Conclusion

The objective of the thesis was to evaluate the axial capacity of cracked tubular elements analytically and numerically and compare these with laboratory test. This can be divided into a numerical part and an analytical part.

The numerical part was performed in Abaqus where the model had the same geometry as the columns in the experimental work, and three different crack sizes were introduced. To be able to compare the numerical model with the experimental work some conditions had to be in place such as similar boundary conditions and similar buckling shape. Three different linear and non-linear analysis was performed to fit the experimental work as good as possible, one for fitting the boundary conditions and two for matching the buckling shape. The numerical finite element analysis is performed according to DNVGL-RP-C208.

The analytical part was performed according to Norsok N-004. Three different cases were performed here. The boundary conditions for these three cases were the same as for the numerical models. There have been performed a comparison between the experimental work and the Norsok N-004 calculations for the fixed-hinged boundary conditions. In addition to this, the non-linear finite element analysis has been compared with the analytical calculations as well.

- Numerical part: The finite element analysis is compared with the experimental work. The comparison for case 1 (fixed-hinged) show a very good match in the axial capacity results, and the range of the differences are between 2 % to 7 %. The boundary conditions in this numerical model seems to be correct, but the buckling shape is different from the experimental shape. Case 2 and 3 have stiffer and weaker boundary conditions and the buckling shape fits the shapes from the experimental work.
- Analytical part: There is bigger differences between the Norsok N-004 calculations and the experimental works. The axial capacity calculations performed with Norsok N-004 formulas for an undamaged column gives a capacity of 13% lower than the equivalent column in the experimental work. The differences in the comparison between the non-linear analysis and the analytical calculations are almost the same as the comparison for the experimental work and the analytical calculations.

6.2 Suggested further work

Two interesting things to investigate regarding the evaluation of the axial capacity of cracked tubular members in the future would be:

- Introducing spring boundary conditions
- Use the arch length (Riks method) as the non-linear analysis type.

7 References

- [1] S. P. Timoshenko and J. M. Gere, "Elastic Buckling of Bars and Frames" in Theory of elastic stability, 2. ed., McGraw-Hill international book company, 1985, pp. 1, 46.
- [2] A. P. Boresi and R. J. Schmidt, Elastic and inelastic stability of columns, in Advanced mechanics of materials, 6 ed., New York: Wiley, 2003, pp. 424-425.
- [3] A. Robertson, "The strength of struts," *Selected Engineering Papers*, no. 28, 1925.
- [4] T. M. Vo, K. Hestholm, G. Ersdal, N. Oma and M. Sivertsvik, "Buckling capacity of simulated patch corroded tubular columns – laboratory tests," *IOP Conference Series: Materials Science and Engineering*, no. 1, 2019.
- [5] J. K. Paik and A. K. Thayamballi, "Collapse Strength of Columns" in Ultimate Limit State Analysis and Design of Plated Structures, 2. ed., John Wiley & Sons, Incorporated, 2018.
- [6] N.-H. Kim, "Nonlinear Finite Element Analysis Procedure" in Introduction to Nonlinear Finite Element Analysis, 1. ed., New York, NY: Springer US, 2015.
- [7] R. D. Cook, D. S. Malkus, M. E. Plesha and R. J. Witt, "Nonlinearity: an introduction" in Concept and applications of finite element analysis, 4. ed., New York: John Wiley & Sons Inc, 2001, pp. 595-598.
- [8] Standard Norge, "Design of steel structures, NORSOK N-004," 2004.
- [9] "Determination of structural capacity by non-linear finite element analysis methods, DNVGL-RP-C208," 2016.
- [10] Dassault Systèmes, "Three-dimensional conventional shell element library," [Online].
] Available:
https://help.3ds.com/2020/english/dssimulia_established/simacaeelmrefmap/simaelm-r-shellgeneral.htm?contextscope=all. [Accessed 12 06 2021].
- [11] S. Riise, "'Experimental evaluation of the axial capacity of cracked tubular members",
] bachelor thesis," 2021.
- [12] S. K. Chakrabarti, "Floating Offshore Platform Design" in Handbook of Offshore
] Engineering (2-Volume Set), St. Louis: Elsevier Science & Technology, 2005, p. 619.

- [13 Tibnor, “Handelsrør EN 10217-1,” [Online]. Available:
] https://www.tibnor.no/nb_NO/Karbonst%C3%A5l/R%C3%B8r/R%C3%B8r/Handelsr%C3%B8r-EN-10217-1/p/506001005616. [Accessed 12 06 2021].

Appendix A Hand calculations with Norsok N-004

Hand calculations of Capacity of cracked tubular

Done with formulas in Norsok N-004 [8] and some formulas from Simen Riise [11].

Constants

```
Ce = 0.3; %Critical elastic buckling coefficient
t = 2.9; %"wall-thickness" in mm
r = 35; %radius in mm
D = 2*r; %diameter in mm
l = 1500; %length in mm
k1 = 0.5; %effective length factor for fixed-fixed BC
k2 = 1; %effective length factor for pinned-pinned BC
k3 = 0.7; %effective length factor for fixed-hinged BC
E = 200*10^3; %Young's Modulus in MPA
fy = 370; % Yield stress in MPA
gamma = 1; % Material factor
format short
```

Axial compression 6.3.3 in Norsok N-004

Capacity calculation on an undamaged tubular column.

Characteristic elastic local buckling strength:

$$f_{cle} = \frac{2C_e E t}{D}$$

```
fcle = (2*Ce*E*t)/(D)
```

```
fcle = 4.9714e+03
```

Norsok N-004 [8] 6.3.3, equation (6.6 - 6-8), characteristic local buckling strength:

$$f_{cl} = \begin{cases} f_y, & \text{for } \frac{f_y}{f_{cle}} \leq 0.170 \\ \left(1.047 - \frac{0.274 \cdot f_y}{f_{cle}}\right) f_y, & \text{for } 0.170 \leq \frac{f_y}{f_{cle}} \leq 1.911 \\ f_{cle}, & \text{for } \frac{f_y}{f_{cle}} > 1.911 \end{cases}$$

```
fy/fcle
```

```
ans = 0.0744
```

```
fcl = fy
```

```
fcl = 370
```

Norsok N-004 [8] 6.3.3, equation (6.5), column slenderness parameter:

$$\bar{\lambda} = \sqrt{\frac{f_{cl}}{f_E}} = \frac{kl}{\pi i} \sqrt{\frac{f_{cl}}{E}}$$

$$A = 2 \cdot \pi \cdot (r - (t/2)) \cdot t \quad \% \text{Cross sectional area}$$

$$A = 611.3225$$

$$I = (\pi/4) \cdot ((r^4) - (r-t)^4) \quad \% \text{Moment of inertia}$$

$$I = 3.4470e+05$$

$$i = \sqrt{I/A} \quad \% \text{Radius of gyration}$$

$$i = 23.7456$$

$$\text{lambda1} = ((k1 \cdot l) / (\pi \cdot i)) \cdot \sqrt{(f_{cl}) / E}$$

$$\text{lambda1} = 0.4324$$

$$\text{lambda2} = ((k2 \cdot l) / (\pi \cdot i)) \cdot \sqrt{(f_{cl}) / E}$$

$$\text{lambda2} = 0.8649$$

$$\text{lambda3} = ((k3 \cdot l) / (\pi \cdot i)) \cdot \sqrt{(f_{cl}) / E}$$

$$\text{lambda3} = 0.6054$$

NORSOK N-004 [8] 6.3.3, equation (6.3 - 6.4) characteristic axial compressive strength:

$$f_c = \begin{cases} [1.0 - 0.28\bar{\lambda}^2] f_y, & \text{for } \bar{\lambda} \leq 1.34 \\ \frac{0.9 \cdot f_y}{\bar{\lambda}^2}, & \text{for } \bar{\lambda} \geq 1.34 \end{cases}$$

$$f_{c1} = (1 - 0.28 \cdot (\text{lambda1}^2)) \cdot f_y$$

$$f_{c1} = 350.6274$$

$$f_{c2} = (1 - 0.28 \cdot (\text{lambda2}^2)) \cdot f_y$$

$$f_{c2} = 292.5094$$

$$f_{c3} = (1 - 0.28 \cdot (\text{lambda3}^2)) \cdot f_y$$

$$f_{c3} = 332.0296$$

NORSOK N-004 6.3.3 [8], equation (6.2), design axial compressive resistance:

$$N_{sd} \leq N_{dent,c,Rd} = \frac{N_{dent,c}}{\gamma_M}, \quad (3.6)$$

%Design axial compressive resistance (effective length factor k1 = 0.5, fixed-fixed)

$$NcRd1 = (A*fc1)/\gamma$$

$$NcRd1 = 2.1435e+05$$

%Design axial compressive resistance (effective length factor k2 = 1, pinned-pinned)

$$NcRd2 = (A*fc2)/\gamma$$

$$NcRd2 = 1.7882e+05$$

%Design axial compressive resistance (effective length factor k3 = 0.7, fixed-hinged)

$$NcRd3 = (A*fc3)/\gamma$$

$$NcRd3 = 2.0298e+05$$

Dented tubular members, axial compression, NORSOK N-2004, (10.6.2.2)

$$c1 = 0.88;$$

$$c2 = 0.765;$$

$$c3 = 0.615;$$

$$c4 = 1;$$

$$Ac1 = t*(r-(t/2))*(2*pi*(1-c1)) \quad \%Crack \text{ area, } 12\% \text{ crack}$$

$$Ac1 = 73.3587$$

$$Ac2 = t*(r-(t/2))*(2*pi*(1-c2)) \quad \%Crack \text{ area, } 23,5\% \text{ crack}$$

$$Ac2 = 143.6608$$

$$Ac3 = t*(r-(t/2))*(2*pi*(1-c3)) \quad \%Crack \text{ area, } 38,5\% \text{ crack}$$

$$Ac3 = 235.3592$$

$$Ac4 = t*(r-(t/2))*(2*pi*(1-c4)) \quad \%Crack \text{ area, } 0\% \text{ crack}$$

$$Ac4 = 0$$

NORSOK N-004 [8] (10.7.2), equation 10.10, dent depth:

$$\bar{\delta} = \frac{1}{2} \cdot \left(1 - \cos \pi \frac{A_{crack}}{A} \right) \cdot D$$

$$\delta_{1} = (1/2)*(1-\cos((\pi*Ac1)/A))*D \quad \%Dent \text{ depth for } 12\% \text{ crack}$$

$$\delta_{1} = 2.4578$$

$$\delta_{2} = (1/2)*(1-\cos((\pi*Ac2)/A))*D \quad \%Dent \text{ depth for } 23,5\% \text{ crack}$$

$$\delta_{2} = 9.1129$$

$$\text{delta3} = (1/2) * (1 - \cos((\pi * A c_3) / A)) * D \quad \% \text{Dent depth for 38,5\% crack}$$

$$\text{delta3} = 22.6284$$

$$\text{delta4} = (1/2) * (1 - \cos((\pi * A c_4) / A)) * D \quad \% \text{Dent depth for 0\% crack}$$

$$\text{delta4} = 0$$

NORSOK N-004 [8], equation (10.4), correction factor for axial resistance:

$$\xi_C = \exp\left(-0.08 \frac{\delta}{t}\right) \text{ for } \frac{\delta}{t} < 10$$

$$\text{xic1} = \exp(-0.08 * \text{delta1} / t)$$

$$\text{xic1} = 0.9344$$

$$\text{xic2} = \exp(-0.08 * \text{delta2} / t)$$

$$\text{xic2} = 0.7777$$

$$\text{xic3} = \exp(-0.08 * \text{delta3} / t)$$

$$\text{xic3} = 0.5357$$

$$\text{xic4} = \exp(-0.08 * \text{delta4} / t)$$

$$\text{xic4} = 1$$

NORSOK N-004 [8], equation (10.5), correction factor for bending resistance:

$$\xi_M = \exp\left(-0.06 \frac{\delta}{t}\right) \text{ for } \frac{\delta}{t} < 10$$

$$\text{xim1} = \exp(-0.06 * \text{delta1} / t)$$

$$\text{xim1} = 0.9504$$

$$\text{xim2} = \exp(-0.06 * \text{delta2} / t)$$

$$\text{xim2} = 0.8282$$

$$\text{xim3} = \exp(-0.06 * \text{delta3} / t)$$

$$\text{xim3} = 0.6261$$

$$\text{xim4} = \exp(-0.06 * \text{delta4} / t)$$

$$\text{xim4} = 1$$

NORSOK N-004 [8], reduced slenderness of dented member:

$$\bar{\lambda}_d = \sqrt{\frac{N_{dent,c}}{N_{E,dent}}} = \sqrt{\frac{\xi_C}{\xi_M}} \cdot \bar{\lambda}_0$$

$$\lambda_{d11} = (x_{ic1}/x_{im1}) \cdot \lambda_{d1}$$

$$\lambda_{d11} = 0.4252$$

$$\lambda_{d12} = (x_{ic2}/x_{im2}) \cdot \lambda_{d1}$$

$$\lambda_{d12} = 0.4061$$

$$\lambda_{d13} = (x_{ic3}/x_{im3}) \cdot \lambda_{d1}$$

$$\lambda_{d13} = 0.3699$$

$$\lambda_{d14} = (x_{ic4}/x_{im4}) \cdot \lambda_{d1}$$

$$\lambda_{d14} = 0.4324$$

$$\lambda_{d21} = (x_{ic1}/x_{im1}) \cdot \lambda_{d2}$$

$$\lambda_{d21} = 0.8503$$

$$\lambda_{d22} = (x_{ic2}/x_{im2}) \cdot \lambda_{d2}$$

$$\lambda_{d22} = 0.8122$$

$$\lambda_{d23} = (x_{ic3}/x_{im3}) \cdot \lambda_{d2}$$

$$\lambda_{d23} = 0.7399$$

$$\lambda_{d24} = (x_{ic4}/x_{im4}) \cdot \lambda_{d2}$$

$$\lambda_{d24} = 0.8649$$

$$\lambda_{d31} = (x_{ic1}/x_{im1}) \cdot \lambda_{d3}$$

$$\lambda_{d31} = 0.5952$$

$$\lambda_{d32} = (x_{ic2}/x_{im2}) \cdot \lambda_{d3}$$

$$\lambda_{d32} = 0.5685$$

$$\lambda_{d33} = (x_{ic3}/x_{im3}) \cdot \lambda_{d3}$$

$$\lambda_{d33} = 0.5179$$

$$\lambda_{d34} = (x_{ic4}/x_{im4}) \cdot \lambda_{d3}$$

$$\lambda_{d34} = 0.6054$$

NORSOK N-004 [8], equation (10.3), characteristic axial compressive capacity of dented member:

$$N_{dent,c} \left\{ \begin{array}{l} \left(1.0 - 0.28\bar{\lambda}_d^2 \right) \cdot \xi_C \cdot f_y A_0, \text{ for } \bar{\lambda}_d \leq 1.34 \\ \frac{0.9}{\bar{\lambda}_d^2} \cdot \xi_C \cdot f_y A_0, \text{ for } \bar{\lambda}_d > 1.34 \end{array} \right.$$

%Capacity for 12% crack (effective length factor k1 = 0.5, fixed-fixed).
 Ndent11 = (1-(0.28*lamdad11^2))*xic1*fy*A

Ndent11 = 2.0066e+05

%Capacity for 23,5% crack (effective length factor k1 = 0.5, fixed-fixed).
 Ndent12 = (1-(0.28*lamdad12^2))*xic2*fy*A

Ndent12 = 1.6779e+05

%Capacity for 38,5% crack (effective length factor k1 = 0.5, fixed-fixed).
 Ndent13 = (1-(0.28*lamdad13^2))*xic3*fy*A

Ndent13 = 1.1652e+05

%Capacity for 0% crack (effective length factor k1 = 0.5, fixed-fixed).
 Ndent14 = (1-(0.28*lamdad14^2))*xic4*fy*A

Ndent14 = 2.1435e+05

%Capacity for 12% crack (effective length factor k2 = 1, pinned-pinned).
 Ndent21 = (1-(0.28*lamdad21^2))*xic1*fy*A

Ndent21 = 1.6857e+05

%Capacity for 23,5% crack (effective length factor k2 = 1, pinned-pinned).
 Ndent22 = (1-(0.28*lamdad22^2))*xic2*fy*A

Ndent22 = 1.4342e+05

%Capacity for 38,5% crack (effective length factor k2 = 1, pinned-pinned).
 Ndent23 = (1-(0.28*lamdad23^2))*xic3*fy*A

Ndent23 = 1.0259e+05

%Capacity for 0% crack (effective length factor k2 = 1, pinned-pinned).
 Ndent24 = (1-(0.28*lamdad24^2))*xic4*fy*A

Ndent24 = 1.7882e+05

%Capacity for 12% crack (effective length factor k3 = 0.7, fixed-hinged).
 Ndent31 = (1-(0.28*lamdad31^2))*xic1*fy*A

Ndent31 = 1.9039e+05

%Capacity for 23,5% crack (effective length factor k3 = 0.7, fixed-hinged).

$$N_{dent32} = (1 - (0.28 \cdot \lambda_{dad32}^2)) \cdot x_{ic2} \cdot f_y \cdot A$$

$$N_{dent32} = 1.5999e+05$$

%Capacity for 38,5% crack (effective length factor $k_3 = 0.7$, fixed-hinged).

$$N_{dent33} = (1 - (0.28 \cdot \lambda_{dad33}^2)) \cdot x_{ic3} \cdot f_y \cdot A$$

$$N_{dent33} = 1.1206e+05$$

%Capacity for 0% crack (effective length factor $k_3 = 0.7$, fixed-hinged).

$$N_{dent34} = (1 - (0.28 \cdot \lambda_{dad34}^2)) \cdot x_{ic4} \cdot f_y \cdot A$$

$$N_{dent34} = 2.0298e+05$$

Dented tubular members, bending, NORSOK N-2004, (eq. 10.6.2.3)

Design bending moment (M_{Rd}) is given in 6.34.

NORSOK N-004 [8], equation (6.10 - 6.12), characterisitc bending strength:

$$f_m = \begin{cases} \frac{Z}{W} f_y, & \text{for } \frac{f_y D}{Et} \leq 0.0517 \\ \left(1.13 - 2.58 \left(\frac{f_y D}{Et} \right) \left(\frac{Z}{W} \right) \right) f_y, & \text{for } 0.0517 < \frac{f_y D}{Et} \leq 0.1034 \\ \left(0.94 - 0.76 \left(\frac{f_y D}{Et} \right) \left(\frac{Z}{W} \right) \right) f_y, & \text{for } 0.1034 < \frac{f_y D}{Et} \leq 120 \frac{f_y}{E} \end{cases}$$

$$\text{condition} = (f_y \cdot D) / (E \cdot t)$$

$$\text{condition} = 0.0447$$

$$Z = (1/6) \cdot ((D^3) - (D - 2 \cdot t)^3) \quad \text{\%Plastic section modulus}$$

$$Z = 1.3065e+04$$

$$W = I / r \quad \text{\%Modification of elastic section modulus [11].}$$

$$W = 9.8484e+03$$

$$f_m = (Z/W) \cdot f_y$$

$$f_m = 490.8482$$

NORSOK N-004 [8], equation (10.6), design bending capacity of dented section:

$$M_{Sd} \leq M_{dent,Rd} = \begin{cases} \xi_M \cdot M_{Rd}, & \text{if dented area act in compression} \\ M_{Rd}, & \text{otherwise} \end{cases}$$

$$M_{dentRd1} = (f_m \cdot W \cdot x_{im1}) / (\gamma) \quad \text{\%Design bending capacity for 12% crack.}$$

MdentRd1 = 4.5944e+06

```
MdentRd2 = (fm*W*xim2)/(gamma) %Design bending capacity for 23,5% crack.
```

MdentRd2 = 4.0034e+06

```
MdentRd3 = (fm*W*xim3)/(gamma) %Design bending capacity for 38,5% crack.
```

MdentRd3 = 3.0268e+06

```
MdentRd4 = (fm*W*xim4)/(gamma) %Design bending capacity for 0% crack.
```

MdentRd4 = 4.8341e+06

Dented tubular members, combined loading, NORSOK N-2004, (eq. 10.6.2.4)

NORSOK N-004 [8], Euler buckling strength:

$$N_{E, dent} = \pi^2 \frac{EI_{dent}}{(kl)^2}$$

```
%Euler buckling strength for 12% crack (effective length factor k1 = 0.5, fixed-fixed).
```

```
NEdent11 = (pi^2)*(E*I*xim1)/(k1*1)^2
```

NEdent11 = 1.1496e+06

```
%Euler buckling strength for 23,5% crack (effective length factor k1 = 0.5, fixed-fixed).
```

```
NEdent12 = (pi^2)*(E*I*xim2)/(k1*1)^2
```

NEdent12 = 1.0018e+06

```
%Euler buckling strength for 38,5% crack (effective length factor k1 = 0.5, fixed-fixed).
```

```
NEdent13 = (pi^2)*(E*I*xim3)/(k1*1)^2
```

NEdent13 = 7.5739e+05

```
%Euler buckling strength for 0% crack (effective length factor k1 = 0.5, fixed-fixed).
```

```
NEdent14 = (pi^2)*(E*I*xim4)/(k1*1)^2
```

NEdent14 = 1.2096e+06

```
%Euler buckling strength for 12% crack (effective length factor k1 = 1, pinned-pinned).
```

```
NEdent21 = (pi^2)*(E*I*xim1)/(k2*1)^2
```

NEdent21 = 2.8741e+05

```
%Euler buckling strength for 23,5% crack (effective length factor k1 = 1, pinned-pinned).
```

$$NEdent22 = (\pi^2)*(E*I*xim2)/(k2*1)^2$$

$$NEdent22 = 2.5044e+05$$

%Euler buckling strength for 38,5% crack (effective length factor k1 = 1, pinned-pinned).

$$NEdent23 = (\pi^2)*(E*I*xim3)/(k2*1)^2$$

$$NEdent23 = 1.8935e+05$$

%Euler buckling strength for 0% crack (effective length factor k1 = 1, pinned-pinned).

$$NEdent24 = (\pi^2)*(E*I*xim4)/(k2*1)^2$$

$$NEdent24 = 3.0240e+05$$

%Euler buckling strength for 12% crack (effective length factor k3 = 0.7, fixed-hinged).

$$NEdent31 = (\pi^2)*(E*I*xim1)/(k3*1)^2$$

$$NEdent31 = 5.8655e+05$$

%Euler buckling strength for 23,5% crack (effective length factor k3 = 0.7, fixed-hinged).

$$NEdent32 = (\pi^2)*(E*I*xim2)/(k3*1)^2$$

$$NEdent32 = 5.1110e+05$$

%Euler buckling strength for 38,5% crack (effective length factor k3 = 0.7, fixed-hinged).

$$NEdent33 = (\pi^2)*(E*I*xim3)/(k3*1)^2$$

$$NEdent33 = 3.8642e+05$$

%Euler buckling strength for 0% crack (effective length factor k3 = 0.7, fixed-hinged).

$$NEdent34 = (\pi^2)*(E*I*xim4)/(k3*1)^2$$

$$NEdent34 = 6.1714e+05$$

$$h = 4 \quad \% \text{Hole size in mm}$$

$$h = 4$$

thethah = h/r
[11].
%Hole size converted to radians

$$thethah = 0.1143$$

$$Ah = t*(r-(t/2))*thethah \quad \% \text{Area of hole}$$

$$Ah = 11.1194$$

```
%Centroided holes relative to original N.A (Crack 12%)[2].  
yh1 = ((t-2*r)*(sin((pi*(1-c1))-thethah)-sin(pi*(1-c1))))/(2*thethah)
```

```
yh1 = 31.8311
```

```
%Distance between original N.A and sections with holes N.A (crack 12%) [11].  
eh1 = (2*Ah*yh1)/(A-(2*Ah))
```

```
eh1 = 1.2017
```

```
% Centroided holes relative to original N.A (Crack 23,5%) [11].  
yh2 = ((t-2*r)*(sin((pi*(1-c2))-thethah)-sin(pi*(1-c2))))/(2*thethah)
```

```
yh2 = 26.0495
```

```
%Distance between original N.A and sections with holes N.A (crack 23,5%)  
[11].  
eh2 = (2*Ah*yh2)/(A-(2*Ah))
```

```
eh2 = 0.9834
```

```
% Centroided holes relative to original N.A (Crack 38,5%) [11].  
yh3 = ((t-2*r)*(sin((pi*(1-c3))-thethah)-sin(pi*(1-c3))))/(2*thethah)
```

```
yh3 = 13.6247
```

```
%Distance between original N.A and sections with holes N.A (crack 38,5%)  
[11].  
eh3 = (2*Ah*yh3)/(A-(2*Ah))
```

```
eh3 = 0.5144
```

```
% Centroided holes relative to original N.A (Crack 0%) [11].  
yh4 = ((t-2*r)*(sin((pi*(1-c4))-thethah)-sin(pi*(1-c4))))/(2*thethah)
```

```
yh4 = 33.4770
```

```
%Distance between original N.A and sections with holes N.A (crack 0%) [11].  
eh4 = (2*Ah*yh4)/(A-(2*Ah))
```

```
eh4 = 1.2638
```

```
%Eccentricity due to holes and initial out of straightness (crack 12%) [11].  
deltay21 = eh1+(1/2000)
```

```
deltay21 = 1.9517
```

```
%Eccentricity due to holes and initial out of straightness (crack 23,5%)  
[11].  
deltay22 = eh2+(1/2000)
```

```
deltay22 = 1.7334
```

```
%Eccentricity due to holes and initial out of straightness (crack 38,5%) [11]
deltay23 = eh3+(1/2000)
```

```
deltay23 = 1.2644
```

```
%Eccentricity due to holes and initial out of straightness (crack 38,5%) [11]
deltay24 = eh4+(1/2000)
```

```
deltay24 = 2.0138
```

NORSOK N-004 [8], equation (10.8):

$\alpha = 2 - 3 \left(\frac{\delta}{D} \right)$, if dented area act in compression

```
alpha1 = 2-(3*(delta1/D))
```

```
alpha1 = 1.8947
```

```
alpha2 = 2-(3*(delta2/D))
```

```
alpha2 = 1.6094
```

```
alpha3 = 2-(3*(delta3/D))
```

```
alpha3 = 1.0302
```

```
alpha4 = 2-(3*(delta4/D))
```

```
alpha4 = 2
```

NORSOK N-004 [8], equation (10.7), design axial force on the dented section:

$$\frac{N_{Sd}}{N_{dent,c,Rd}} + \sqrt{\left(\frac{N_{Sd}\Delta y_2 + C_{m1}M_{1,Sd}}{\left(1 - \frac{N_{Sd}}{N_{E,dent}}\right)M_{dent,Rd}} \right)^\alpha} \leq 1$$

```
syms NSd
```

```
%Design axial force for 12% crack, combined effect,
%(effective length factor k1 = 0.5, fixed-fixed).
```

```
eqn1 = (NSd/Ndent11) + (sqrt((NSd*deltay21)/((1-
(NSd/(NEdent11))*MdentRd1))^alpha1)-1;
```

```
eqns1 = vpasolve(eqn1,NSd);
```

```
eq1 = eqns1*10^-3
```

```
eq1 = 180.01812611800476255341182806252
```

```
%Design axial force for 23,5% crack, combined effect,
%(effective length factor k1 = 0.5, fixed-fixed).
```

```
eqn2 = (NSd/Ndent12) + (sqrt((NSd*deltay22)/((1-
(NSd/NEdent12))*MdentRd2))^alpha2) -1;
```

```
eqns2 = vpasolve(eqn2,NSd);  
eq2 = eqns2*10^-3
```

eq2 = 147.0097240674611691694300302448

```
%Design axial force for 38,5% crack, combined effect,  
%(effective length factor k1 = 0.5, fixed-fixed).  
eqn3 = (NSd/Ndent13) + (sqrt((NSd*deltay23)/((1-  
(NSd/NEdent13))*MdentRd3))^alpha3) -1;  
eqns3 = vpasolve(eqn3,NSd);  
eq3 = eqns3*10^-3
```

eq3 = 93.111236261615159700186058963745

```
%Design axial force for 12% crack, combined effect,  
%(effective length factor k2 = 1, pinned-pinned).  
eqn4 = (NSd/Ndent21) + (sqrt((NSd*deltay21)/((1-  
(NSd/NEdent21))*MdentRd1))^alpha1) -1;  
eqns4 = vpasolve(eqn4,NSd);  
eq4 = eqns4*10^-3
```

eq4 = 145.14014603508375070168496178954

```
%Design axial force for 23,5% crack, combined effect,  
%(effective length factor k2 = 1, pinned-pinned).  
eqn5 = (NSd/Ndent22) + (sqrt((NSd*deltay22)/((1-  
(NSd/NEdent22))*MdentRd2))^alpha2) -1;  
eqns5 = vpasolve(eqn5,NSd);  
eq5 = eqns5*10^-3
```

eq5 = 120.7597813125862411812676210119

```
%Design axial force for 38,5% crack, combined effect,  
%(effective length factor k2 = 1, pinned-pinned).  
eqn6 = (NSd/Ndent23) + (sqrt((NSd*deltay23)/((1-  
(NSd/NEdent23))*MdentRd3))^alpha3) -1;  
eqns6 = vpasolve(eqn6,NSd);  
eq6 = eqns6*10^-3
```

eq6 = 79.170299229040579161280472114423

```
%Design axial force for 12% crack, combined effect,  
%(effective length factor k3 = 0.7, fixed-hinged).  
eqn7 = (NSd/Ndent31) + (sqrt((NSd*deltay21)/((1-  
(NSd/NEdent31))*MdentRd1))^alpha1) -1;  
eqns7 = vpasolve(eqn7,NSd);  
eq7 = eqns7*10^-3
```

eq7 = 168.76725497903413549850745937543

```

%Design axial force for 23,5% crack, combined effect,
%(effective length factor k3 = 0.7, fixed-hinged).
eqn8 = (NSd/Ndent32) + (sqrt((NSd*deltay22)/((1-
(NSd/NEdent32))*MdentRd2))^alpha2) -1;
eqns8 = vpsolve(eqn8,NSd);
eq8 = eqns8*10^-3

```

eq8 = 138.54836040872147331979506458009

```

%Design axial force for 38,5% crack, combined effect,
%(effective length factor k3 = 0.7, fixed-hinged).
eqn9 = (NSd/Ndent33) + (sqrt((NSd*deltay23)/((1-
(NSd/NEdent33))*MdentRd3))^alpha3) -1;
eqns9 = vpsolve(eqn9,NSd);
eq9 = eqns9*10^-3

```

eq9 = 88.606047938350632679404557231353

```

%Design axial force for 0% crack, combined effect,
%(effective length factor k1 = 0.5, fixed-fixed).
eqn100 = (NSd/Ndent14) + (sqrt((NSd*deltay24)/((1-
(NSd/NEdent14))*MdentRd4))^alpha4) -1;
eqns100 = vpsolve(eqn100,NSd);
eq100 = eqns100*10^-3

```

eq100 = $\begin{pmatrix} 193.74654027475294034922243984605 \\ 1338.2133397810838310634800744711 \end{pmatrix}$

```

%Design axial force for 0% crack, combined effect,
%(effective length factor k2 = 1, pinned-pinned).
eqn101 = (NSd/Ndent24) + (sqrt((NSd*deltay24)/((1-
(NSd/NEdent24))*MdentRd4))^alpha4) -1;
eqns101 = vpsolve(eqn101,NSd);
eq101 = eqns101*10^-3

```

eq101 = $\begin{pmatrix} 155.09865217650672730042709960879 \\ 348.64656565112927561138189725078 \end{pmatrix}$

```

%Design axial force for 0% crack, combined effect,
%(effective length factor k3 = 0.7, fixed-hinged).
eqn103 = (NSd/Ndent34) + (sqrt((NSd*deltay24)/((1-
(NSd/NEdent34))*MdentRd4))^alpha4) -1;
eqns103 = vpsolve(eqn103,NSd);
eq103 = eqns103*10^-3

```

eq103 = $\begin{pmatrix} 181.27433373516355595794826207361 \\ 691.03168181524822014602656956034 \end{pmatrix}$

References

[8] Standard Norge, *Design of steel structures*, NORSOK N-004, 2004.

[11] S. Riise, «"Experimental evaluation of the axial capacity of cracked tubular members", bachelor thesis,» 2021.